



MSc thesis in Biotechnology

Harnessing Sorghum's Root Exudate Metabolism for Sustainable Agriculture

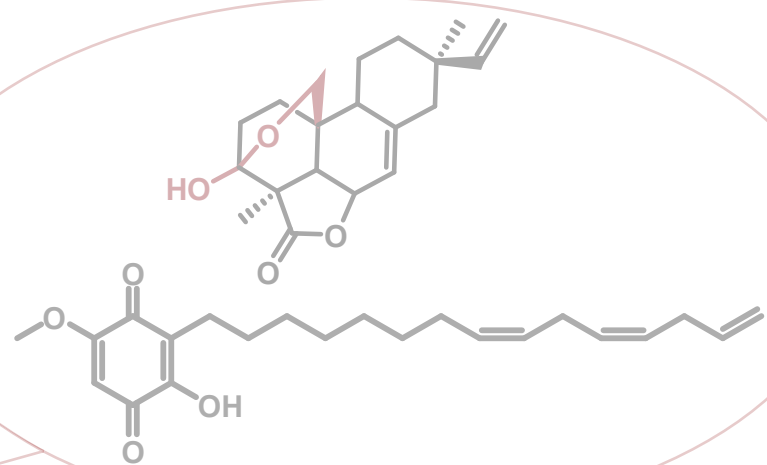
Biosynthetic and Regulatory Insights into Allelopathic and Nitrification-Inhibiting Metabolites

Jens Sigurd Agger Raabyemagle

Supervised by Tomas Laursen, Kasper Hinz, William Thomas Wajn,

and Johan Andersen-Ranberg

October 2025



Jens Sigurd Agger Raabyemagle

Harnessing Sorghum's Root Exudate Metabolism for Sustainable Agriculture

MSc thesis in Biotechnology, October 2025

Supervisors: Tomas Laursen, Kasper Hinz, William Thomas Wajn, and Johan Andersen-Ranberg

University of Copenhagen

Faculty of Science

Department of Plant and Environmental Sciences

Masters Degree in Biotechnology

Thorvaldsensvej 40

1871 Frederiksberg



"I like the scientific spirit—the holding off, the being sure but not too sure, the willingness to surrender ideas when the evidence is against them: this is ultimately fine—it always keeps the way beyond open—always gives life, thought, affection, the whole man, a chance to try over again after a mistake—after a wrong guess."

- Walt Whitman

"It seems to me that the natural world is the greatest source of excitement; the greatest source of visual beauty; the greatest source of intellectual interest. It is the greatest source of so much in life that makes life worth living"

- Sir David Attenborough

Preface

This thesis marks the conclusion of my Master's studies in Biotechnology at the University of Copenhagen and was carried out at the Department of Plant and Environmental Sciences under the primary supervision of Tomas Laursen. The work was conducted within the framework of the Dynamic Metabolons research group and explores the biosynthesis, regulation, and evolutionary context of allelochemical and biological nitrification inhibitor compounds in *Sorghum bicolor*.

The project was motivated by a long-standing interest in how plants use specialized metabolism to adapt to their environment and how this chemistry can be harnessed for more sustainable agriculture. Throughout the project, I was fortunate to work at the interface of molecular biology, analytical chemistry, and plant biochemistry fields that together reveal how molecular diversity translates into ecological function. Much of this work was experimental in nature, involving cloning, transient expression in *Nicotiana benthamiana*, metabolite analysis using GC-MS, and comparative interpretation of pathway evolution between species. Like most research, progress came with both breakthroughs and setbacks, each shaping a deeper understanding of the complexity of plant metabolism and analytical chemistry.

I am deeply grateful to my supervisors for their guidance, inclusion, and encouragement throughout the project, and to my colleagues and friends in the lab for their support, stimulating discussions, and good company during long days of cloning, peak picking, and writing. Finally, I would like to thank my family and partner for their patience and for always reminding me of the bigger picture.

List of Abbreviations

A. tumefaciens *Agrobacterium tumefaciens*

ARS Alkylresorcinol synthase

BNI Biological Nitrification Inhibitor

BSTFA N,O-Bis(trimethylsilyl)-trifluoroacetamide

CoA Coenzyme A

CPS Copalyl diphosphate synthase

CYP Cytochrome P450 monooxygenase

Cytb₅ Cytochrome b₅

DDT Dichlorodiphenyltrichloroethane

DES Fatty acid desaturase

DNA Deoxyribonucleic acid

dNTPs Deoxynucleotide triphosphates

ED₈₀ Effective dose inhibiting 80% of population

GC–MS Gas Chromatography–Mass Spectrometry

Gent Gentamicin

GFP Green fluorescent protein

GGOH Geranylgeraniol

GGPP Geranylgeranyl pyrophosphate

IS Internal standard

I₅₀ Inhibitory concentration causing 50% inhibition

Kan Kanamycin

KSL Kaurene synthase-like enzyme

LACS Long-chain acyl-CoA synthetase

LB Luria-Bertani

MAS Momilactone A synthase

MEP pathway Methylerythritol phosphate pathway

MES 2-(N-Morpholino)ethanesulfonic acid

MSBP Membrane steroid-binding protein
MVA pathway Mevalonate pathway
m/z Mass-to-charge ratio
N. benthamiana *Nicotiana benthamiana*
OD₆₀₀ Optical density at 600 nm
OMT O-methyltransferase
Os/rice *Oryza sativa*
p19 Gene silencing suppressor from *Tomato bushy stunt virus*
PCR Polymerase Chain Reaction
PTGS Post-transcriptional gene silencing
Rif Rifampicin
RNAi RNA interference
RT-qPCR Reverse transcriptase quantitative polymerase chain reaction
Sb/Sorghum *Sorghum bicolor*
SNI Synthetic Nitrification Inhibitor
SOC Super optimal catabolite
T-DNA Transfer DNA
TIC Total Ion Chromatogram
USER Uracil-specific excision reagent
YEP Yeast extract and peptone
2,4-D 2,4-dichlorophenoxyacetic acid

Abstract

Plants produce a vast array of specialized metabolites that mediate ecological interactions and influence nutrient cycling in the rhizosphere. This thesis investigates the biosynthesis and regulation of two such metabolites in *Sorghum bicolor*, namely the labdane-type diterpenoid allelochemical momilactone B, and the lipophilic resorcinol-type biological nitrification inhibitor (BNI) sorgoleone. Both compounds exemplify how plants chemically adapt to environmental pressures and regulate belowground processes such as weed suppression and microbial competition.

In the first case study, it was hypothesized that sorghum possesses functional orthologs to the rice momilactone B biosynthetic genes, reflecting conservation of this ancestral diterpenoid pathway. To test this, the rice pathway was first reconstituted in *Nicotiana benthamiana*, confirming its functionality in this heterologous host. Systematic replacement of individual rice genes with their sorghum counterparts revealed partial functional conservation. Several sorghum enzymes, including SbKSL4, SbCYP76M8/14, and SbMAS, catalyzed expected intermediates but failed to restore full momilactone B biosynthesis. The results suggested that while catalytic traits have been retained, the complete pathway has diverged functionally in sorghum, consistent with genomic evidence of an ancestral momilactone gene cluster that has likely since specialized toward related diterpenoid metabolism. The second case study tested the hypothesis that the sorgoleone biosynthetic pathway could similarly be reconstructed in *N. benthamiana*, and that co-expression of candidate regulatory or accessory proteins (SbMSBP1, SbCytb_{5,6}, and SbLACS4.1) identified in sorghum root hair proteomics might enhance or stabilize pathway activity. However, neither pathway intermediates nor phenotypic effects were detected, suggesting that expression was unsuccessful, likely due to post-transcriptional silencing or incomplete transgene expression.

Together, these studies highlight both the potential and the limitations of using transient plant expression systems for comparative pathway reconstruction. They provide new insight into the functional diversity of sorghum enzymes, and identify key methodological and regulatory bottlenecks that must be addressed for successful heterologous reconstitution of complex plant secondary metabolic pathways.

Contents

1	Introduction	1
1.1	Plant secondary metabolism in the context of modern agriculture	1
1.2	Plant BNIs and allelochemicals	4
1.3	Case study 1: Momilactone B	7
1.4	Case study 2: Sorgoleone	9
1.4.1	Potential regulatory elements supporting sorgoleone biosynthesis	12
2	Thesis Scope and Rationale	13
3	Materials and Methods	15
3.1	Bioinformatic identification of sorghum orthologs	15
3.2	Generation of plant expression vectors by USER cloning	16
3.2.1	Preparation of vector backbone	17
3.2.2	Preparation of DNA inserts, and cloning reactions	17
3.3	Transient expression of biosynthetic pathways in <i>Nicotiana benthamiana</i>	19
3.3.1	Metabolic engineering steps for momilactone B precursor boost	19
3.3.2	Transformation of <i>Agrobacterium tumefaciens</i>	19
3.3.3	Agroinfiltration of <i>Nicotiana benthamiana</i>	20
3.4	Metabolite extraction	21
3.5	Gas chromatography - mass spectrometry	22
3.5.1	Momilactone B detection method	22
3.5.2	Sorgoleone detection method	22
4	Results	25
4.1	Case study 1: Momilactone B	25
4.1.1	Experimental setup	25
4.1.2	Expression of rice biosynthetic genes in <i>N. benthamiana</i>	25
4.1.3	Functional complementation with sorghum ortholog genes	30
4.2	Case study 2: Sorgoleone	34
4.2.1	Experimental setup	34

4.2.2 Expression of sorgoleone biosynthetic genes and potential regulators in <i>N. benthamiana</i>	35
5 Discussion	37
5.1 Evaluating <i>N. benthamiana</i> as a heterologous transient expression host	37
5.2 Evolution of momilactone biosynthetic gene clusters with respect to sorghum	40
5.3 Experimental setup of sorgoleone pathway expression	42
6 Conclusion	45
7 Perspectives	47
8 Bibliography	49
9 Appendix	57

Introduction

1.1 Plant secondary metabolism in the context of modern agriculture

Synthetic agrochemicals, encompassing both pesticides and fertilizers, have profoundly shaped modern agricultural practices. The invention of the Haber-Bosch process in the early 20th century allowed for the industrialized fixation of atmospheric nitrogen into ammonia, providing the foundation for production of synthetic fertilizers that dramatically improved global crop yields (Smil, 2001). Following the Second World War, chemical pest control was similarly revolutionized by the industrial production and widespread adoption of synthetic pesticides such as dichlorodiphenyltrichloroethane (DDT) (Turusov *et al.*, 2002). At the same time, discovery and commercialization of synthetic chemical herbicides permitted effective widespread combating of leafy weeds with products such as 2,4-dichlorophenoxyacetic acid (2,4-D) (Peterson *et al.*, 2016). These innovations underpinned the so-called Green Revolution, driving unprecedented increases in global food production as well as decreases in food prices, which helped to sustain the rapidly growing global population (Pingali, 2012).

Despite the transformative successes of the Green Revolution, the reliance on high-input agricultural systems has brought several environmental challenges with it. There are numerous reports on the health risks to humans posed by the long-term use and exposure to synthetic pesticides, including cancer, DNA damage, neurologic disorders, respiratory impairment, and metabolic diseases (Curl *et al.*, 2020). Similarly, 2,4-D has also been reported to have many off-target effects on the environment, due to its persistence in the environment and its bioactivity (Castro Marcato *et al.*, 2017). The use of synthetic ammonia-based fertilizers has also proven detrimental to the environment. When ammonia is applied to soil, it is not only used as a source of energy for the crops for which it is intended, but also for several rhizosphere microorganisms. Ammonium from the fertilizer is oxidized to nitrate by several chemolithoautotrophic bacteria and archaea in a two-step reaction termed nitrification (Beeckman *et al.*, 2018). While nitrate inherently also can be absorbed as a nutrient by plants, its higher mobility

in soil leads to faster leaching into the broader environment. This leaching causes contamination of ground- and surface-water, as well as causing eutrophication, where nitrate feeds harmful algal blooms that deplete water oxygen levels resulting in loss of aquatic life (Arend *et al.*, 2011; Glibert *et al.*, 2005). Nitrate can also be used as a source of energy for denitrifying bacteria, producing the potent greenhouse gas nitrous oxide, which contributes to global warming (Tian *et al.*, 2020). The documented environmental and health hazards of high-input agriculture underscore the need to critically re-evaluate the chemical inputs that underpin modern farming systems. This is emphasized by both the United Nations Sustainable Development Goal 2 (United Nations, 2025) and the European Union Green Deal calling for 50% reduction in pesticide use (European Commission, 2025).

An alternative strategy to maintain the efficacy of agricultural chemical inputs, while mitigating environmental damage, is to harness the chemical diversity already present in plants themselves. Plants, being sessile organisms, have through millions of years co-evolved with their environment to produce a chemical arsenal that mediate interactions with pathogens, pests, competitors, and symbiotic organisms (Ono and Murata, 2023; Jahan *et al.*, 2025). These natural compounds are termed secondary metabolites, stemming from primary metabolite production but evolved towards very specific purposes. Examples include flavonoid phytoalexins that accumulate in plant tissue in response to fungal infection (Ube *et al.*, 2021), volatile sesquiterpenoids that repel disease-spreading insects through smell (Alquézar *et al.*, 2017), allelopathic diterpenes that inhibit the growth of neighboring plants that compete for nutrition (Kato-Noguchi, 2023), and colorful anthocyanins that attract pollinators vital for reproduction (Trunschke *et al.*, 2021) (Figure 1). Unlike synthetic agrochemicals, plant-derived compounds are generally thought to be biodegradable and tailored to the complexity of the biological systems within the environment they are released to (Schütz *et al.*, 2021). Exploring such metabolites as potential substitutes or complements to conventional agricultural inputs thus represents a promising road towards reducing the environmental footprint of agriculture, while still maintaining productivity.

Sorghum bicolor (sorghum) is a great example of a plant, which has adapted to its environment through secondary metabolism. As one of the worlds most stress-tolerant cereals, sorghum thrives in nutrient-poor and drought-prone soils (Mwamahonje *et al.*, 2021) while producing an exceptionally rich array of secondary metabolites, including cyanogenic glycosides (Halkier and Lindberg Møller, 1989), flavonoids (Dykes *et al.*, 2009), and lipid benzoquinones (Subbarao *et al.*, 2013). Many of these compounds

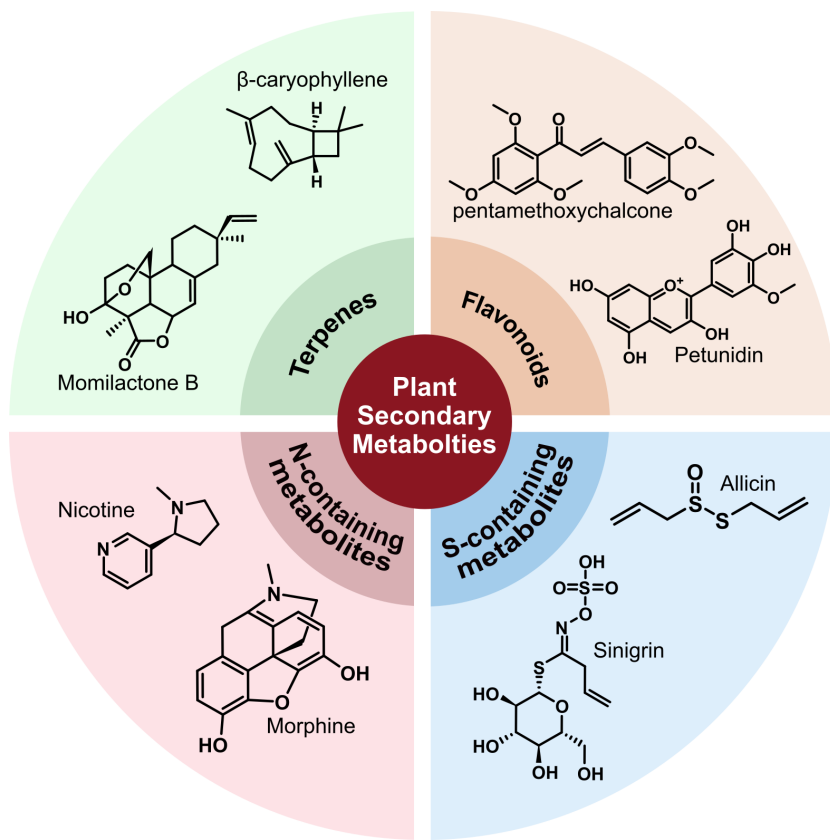


Figure 1: Diversity of plant secondary metabolites.

mediate interactions with pathogens, herbivores, and neighboring plants, underscoring the role of metabolic innovation in environmental adaptation. This chemical versatility has also made sorghum a leading model for exploring how plant metabolites can be leveraged to enhance nutrient efficiency and natural weed suppression, which are key goals in the transition toward more sustainable agroecosystems.

1.2 Plant BNIs and allelochemicals

Among the many ecological roles of plant secondary metabolites, two are particularly relevant for agriculture: allelopathy and biological nitrification inhibition (BNI). With allelopathic compounds, plants release metabolites that suppress the germination or growth of neighboring species, reducing competition for nutrients and light (Bajwa, 2014). In a similar way, BNIs act in the soil by inhibiting the microorganisms that drive nitrification, thereby retaining available nitrogen in a plant-preferred state (Beeckman *et al.*, 2018). Both mechanisms illustrate how plant-derived chemistry can address the same challenges that synthetic herbicides and fertilizers were designed for, but in a way that is naturally integrated into ecological interactions and nutrient cycling (figure 2).

The concept of BNI refers to the release of secondary metabolites that directly suppress the activity of ammonia-oxidizing microorganisms in the rhizosphere, thereby ensuring uptake of available ammonia in the soil. Early characterization of BNI activity was achieved through bioluminescence-assays targeting the model ammonia-oxidizing bacteria *Nitrosomonas europaea*, which provided quantitative evidence that plant root exudates can interfere with the first step of nitrification (Subbarao *et al.*, 2006). This approach enabled the identification of brachialactone in the tropical forage grass *Brachiaria humidicola*, a unique cyclic diterpenoid lactone with activity comparable to the synthetic nitrification inhibitor (SNI) nitrapyrin (Subbarao *et al.*, 2009). Such findings confirmed that specialized plant metabolites can act on key microbial processes in the rhizosphere with efficacy on par with synthetic agrochemicals.

As research progressed, the scope of BNI investigations expanded beyond tropical forage grasses to include cereals and other crops, since genetic efforts to increase endogenous BNI production in crops are at the heart of what BNI research aims to achieve. A growing body of work has revealed a chemically diverse set of metabolites with BNI activity, ranging from benzoxazinoids such as zeanone in *Zea mays* (Otaka *et al.*, 2022), to fatty alcohols such as 1,9-decanediol in *Oryza sativa* (rice) (Lu *et al.*, 2022), as well as other yet to be characterized BNIs in *Triticum aestivum* (Subbarao *et al.*, 2007). This diversity indicates that BNI is not restricted to a single compound class or biosynthetic origin, but rather represents a convergent ecological strategy in plants to modulate the nitrogen cycle in their immediate environment.

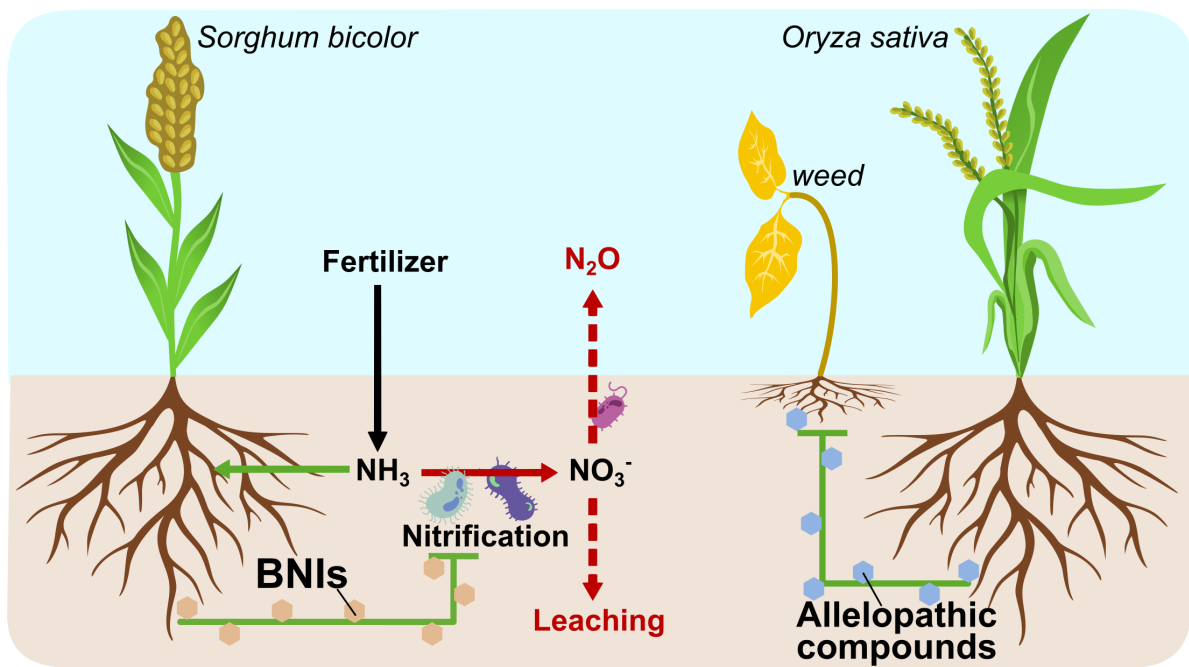


Figure 2: Illustration of BNI and allelopathic activity. Soil microorganisms oxidize ammonia to nitrate, which in turn can leach into waterways, or be subject to denitrification which produces the greenhouse gas N_2O . BNIs from e.g. sorghum inhibit the bacteria and archaea responsible for nitrification, thereby retaining ammonia in the soil. Allelopathic compounds from e.g. rice can inhibit weeds that otherwise compete for nutrients and sunlight.

Beyond compounds with BNI activity, many plants have been found to release a broad spectrum of allelopathic secondary metabolites that suppress the germination or development of neighboring plants. In the same sense as BNIs, it has been of specific interest to characterize and understand how these compounds are produced and released into the environment by crops, so they can help to make agricultural practices of applying herbicides more sustainable. Examples include the alkaloids hordenine and gramine exuded by *Hordeum vulgare* (Bouhaouel *et al.*, 2015), the benzoxazinoid 5-chloro-6-methoxy-2-benzoxazolinone (DIBOA) from *Z. mays* (Kato-Noguchi *et al.*, 1999), and the coumarin scopoletin from *Avena sativa* (Belz *et al.*, 2005).

Importantly, the methodological framework for BNI and allelopathic research has shifted from simple inhibition assays toward integrative approaches combining metabolite profiling, genetic manipulation, and expression studies in heterologous systems (Ghatak *et al.*, 2025; Kato-Noguchi, 2023; Pan *et al.*, 2021; Egenolf *et al.*, 2023). These advances have provided more precise links between metabolite structure, biosynthetic pathway, and ecological function. As a result, these metabolites are increasingly recognized not as isolated chemical curiosities, but as integral components of plant secondary metabolism with potential agronomic relevance.



Figure 3: Microscopical 80x magnification of a sorghum root, showing exudate droplets on root hairs containing sorgoleone. Figure is from Oliveira *et al.* (2024).

However, to enable targeted genetic manipulation or breeding strategies aimed at enhancing BNI capacity, a comprehensive understanding of both the biosynthesis and regulation of these metabolites is required. At present, only a small number of BNIs and allelochemicals have been fully characterized at the enzymatic and pathway levels, such as the BNI sorgoleone in *Sorghum bicolor* (sorghum) (Pan *et al.*, 2018), and the allelochemical momilactone B in rice (De La Peña and Sattely, 2021). Even in these cases, knowledge is largely restricted to the catalytic sequence of core biosynthetic enzymes, while far less is known about the regulation surrounding their biosynthesis. Another major knowledge gap concerns the spatial and temporal control of metabolite production. Many BNIs are exuded from specific cell types, such as sorghum root hairs in the case of sorgoleone (Figure 3), yet the mechanisms that coordinate pathway enzyme enrichment in these cells remain unclear. Likewise, the environmental triggers that upregulate BNI/allelochemical secretion such as nitrogen availability, microbial presence, plant-plant communication, or abiotic stresses are only beginning to be investigated (Wang *et al.*, 2021; Kumar *et al.*, 2024; Xu *et al.*, 2023). Transport processes also remain a frontier; whether compounds diffuse freely, are exported by dedicated transporters, or accumulate in extracellular vesicles is still poorly understood. Together, these gaps hinder our ability to predict or manipulate BNI activity with respect towards breeding and introgression efforts.

An additional question of high importance is whether BNI-active or allelopathic compounds identified in one species are also produced by other crops. Comparative studies

across plant lineages do not only provide evolutionary insight into how these pathways are regulated, but also offer practical advantages. If a given compound is shared between multiple crops, variation in its regulation across genetic backgrounds may help uncover the underlying control mechanisms. From a plant breeding perspective, the presence of BNIs in staple cereals such as wheat, maize, or sorghum would offer direct routes for selecting or engineering cultivars with improved nitrogen use efficiency or weed suppression capacity. In this way, cross-species investigations are likely to be just as informative for understanding the regulation of BNIs as they are for exploring their ecological and agronomic roles.

1.3 Case study 1: Momilactone B

To explore how specialized metabolites mediate plant–soil interactions, two case studies are examined: momilactone B, a diterpenoid allelochemical from *O. sativa* (rice), and sorgoleone, a benzoquinone exudate from sorghum. Both exemplify how plants integrate complex biosynthetic machinery to modulate competition and nutrient cycling in the rhizosphere. Momilactone B is a cyclic diterpenoid allelochemical originally found to be produced in rice, and later identified in several close relatives of rice as well as in the bryophyte *Calohypnum plumiforme* (Mao *et al.*, 2020). It was initially isolated from the husk of rice grains, but later also found to be exuded by rice roots into the rhizosphere (Kato *et al.*, 1973; Kato-Noguchi *et al.*, 2002). Broad-spectrum reports of allelopathy are derived from several studies characterizing the phytotoxicity of momilactone B in different model and weed plants. Kato-Noguchi *et al.* (2012) examined the dose-dependent inhibition of momilactone B on the hypocotyl and roots of *Arabidopsis thaliana*, a dicotyledon plant, determining the concentration at which plant growth was inhibited by 50% (I_{50}) to be in the low micromolar range of 6.5-12 μM . The same study was conducted to measure the inhibitory effect on the barnyard grass *Echinochloa crus-galli*, a monocotyledon and one of the most detrimental weeds to rice production in the world, where the I_{50} of momilactone B was similarly 6.5-6.9 μM for hypocotyl and roots (Aminpanah *et al.*, 2013; Kato-Noguchi *et al.*, 2010). These effects have spurred a particular interest in leveraging the molecule as a natural herbicide agent in agriculture, wherefrom numerous studies into its biosynthesis have been conducted since.

The biosynthetic pathway of momilactone B in rice is well characterized by several biochemical and genetic studies (Figure 4). The pathway stems from the plastidial

methylerythritol phosphate (MEP) pathway, responsible for the production of isoprenoids. These compounds are crucial in primary metabolism, where they regulate multiple cellular functions, such as the production of ubiquinone involved in respiration, the production of plant hormones such as gibberellins, as well as the diterpene scaffold geranylgeranyl pyrophosphate (GGPP) [1] (Phillips *et al.*, 2008). The biosynthesis of momilactone B in rice starts with the partial cycling of GGPP by the enzyme syn-copalyl diphosphate synthase 4 (OsCPS4) (accessions in table 1) to form syn-copalyl diphosphate [2]. Another cyclase, syn-kaurene synthase-like 4 (OsKSL4), further converts this intermediate into syn-pimara-7,15-diene [3] which is the core hydrocarbon skeleton for momilactone B (Otomo *et al.*, 2004; Xu *et al.*, 2004). The syn-pimaradiene skeleton then undergoes a series of rearrangement and oxidation steps, mainly catalyzed by cytochrome P450 monooxygenase (CYP) enzymes, described in detail by De La Peña and Sattely (2021). They identified the specific CYPs involved by successful expression in and engineering of *Nicotiana benthamiana*, but questioning the sequentialism of their catalyzation (figure 4). One of the possible candidates for the first step is that OsCYP99A3 oxidizes carbon 19 (C19) into syn-pimaradien-19-oic acid [4], which is further oxidized at the C6 position by OsCYP76M8 into 6β -carboxy-synpimaradien-19-oic acid [6]. Alternatively, the reaction occurs in reverse order, where oxidation of C6 happens first making 6β -hydroxy-synpimaradiene [5], with subsequent oxidation at C19 to yield [6]. Momilactone A synthase (OsMAS) forms the lactone ring by combining the C6 carbonyl group with the C19 hydroxyl group, yielding syn-pimaradien-19,6 β -olide [7]. Lastly, another sequence of oxidations is catalyzed by CYP76M14 and CYP701A8 at the C20 and C3 positions, respectively, in a similarly questioned sequence. The oxidation of [7] at C3 yields momilactone A [9], which is also associated with allelopathy, albeit at a much lower efficiency than momilactone B (Kato-Noguchi *et al.*, 2012). These two final oxidations lead to a spontaneous closure of the hemiacetal ring, resulting in momilactone B.

Rice has a dedicated biosynthetic gene cluster for the enzymes responsible for momilactone B biosynthesis on chromosome 4 (Mao *et al.*, 2020), comprising *OsCPS4*, *OsKSL4*, *OsMAS*, and *OsCYP99A3*. The additional oxidative tailoring enzyme genes encoding *OsCYP76M8*, *OsCYP76M14*, and *OsCYP701A8* are localized on chromosome 2, 1, and 6, respectively (Priego-Cubero *et al.*, 2025). This clustering is thought to facilitate coordinated regulation and efficient metabolic flux toward the specialized diterpenoid scaffold. Comparative genomic analyses have revealed that similar clusters, or partial syntenic remnants thereof, are conserved across several *Oryza* species and even occur in more distantly related grasses such as *E. crus-galli* and in the bryophyte *C. plumiforme*, implying an ancient and potentially mobile genomic architecture for this pathway in

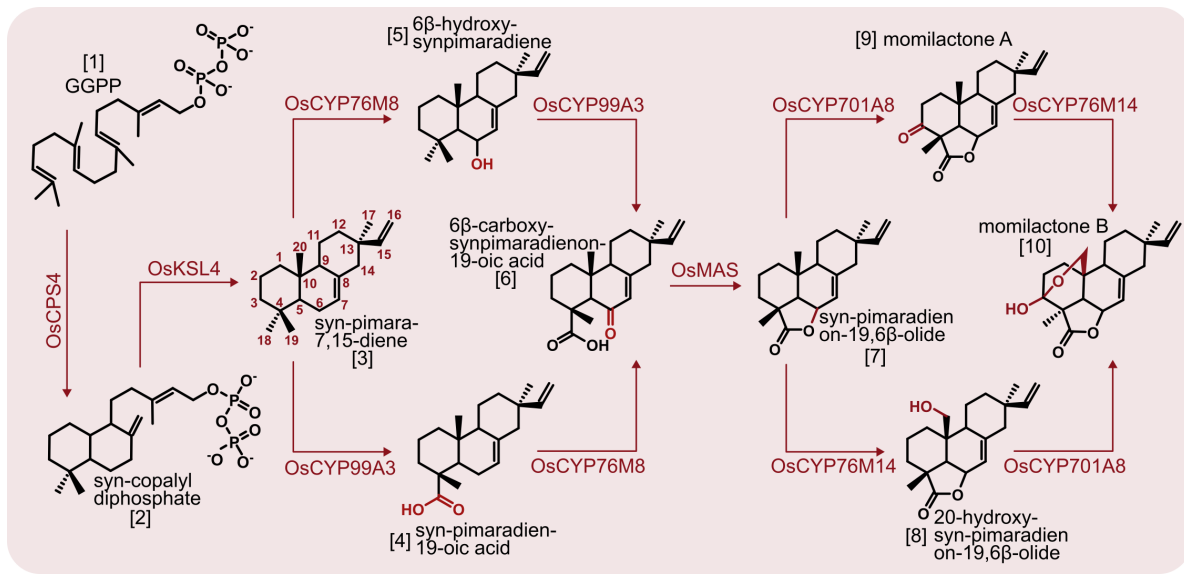


Figure 4: Proposed biosynthesis of momilactone B as described by De La Peña and Sattely (2021).

addition to convergent evolutionary examples (Mao *et al.*, 2020; Priego-Cubero *et al.*, 2025). The presence of momilactone B biosynthetic gene cluster-like gene neighborhoods in multiple lineages suggests that the capacity for momilactone-type metabolism is not unique to rice, motivating exploration of orthologous gene sets in other cereals such as sorghum.

1.4 Case study 2: Sorgoleone

Sorgoleone is a long-chain lipid benzoquinone exuded exclusively from the root hairs of sorghum. It was first identified as the principal allelochemical responsible for the strong weed-suppressing effects of sorghum root exudates, displaying potent inhibition of photosynthetic electron transport and seedling growth in competing plants (Gonzalez *et al.*, 1997). Beyond its established allelopathic activity, sorgoleone has more recently been recognized as a major BNI of sorghum by Subbarao *et al.* (2013), capable of suppressing both ammonia-oxidizing bacteria and archaea in soil, thereby retaining the amount of ammonia present in soils (Okumoto *et al.*, 2025). Subbarao *et al.* (2013) determined that a concentration of 13 µM sorgoleone inhibited 80% (ED_{80}) of the growth of *N. europaea* *in vitro*. These findings position sorgoleone as a central bioactive metabolite in sorghum's chemical ecology, and have prompted numerous research efforts into its biosynthesis and regulatory control.

The biosynthesis of sorgoleone has been extensively investigated over the last two decades, culminating in two suggestions of the entire pathway by Pan *et al.* (2021) and Maharjan *et al.* (2023). The biosynthetic sequence originates from a 16-carbon fatty acid precursor. Pan *et al.* (2021) argues that the commencing precursor is palmitoleoyl-CoA (16:1 Δ^9), an activated fatty acid essential for formation of cell membranes and energy storage (Kalinger *et al.*, 2020). Maharjan *et al.* (2023) argues that the commencing precursor is the palmitoleic acid moiety (16:1 Δ^9) of a membrane lipid such as phosphatidylcholine, a glycerolipid which is the main constituent of plastid outer membranes (figure 5) (Botella *et al.*, 2017). The first step of the pathway is the desaturation of the acyl-chain, first at C12 catalyzed by the fatty acid desaturase SbDES2 to yield hexadecadienoic acid (16:2 $\Delta^{9,12}$), which is further desaturated by SbDES3 to yield hexadecatrienoic acid (16:3 $\Delta^{9,12,15}$). Maharjan *et al.* (2023) argues that there is an unknown mechanism releasing the hexadecatrienoic acid moiety from the modified phaspahtidylcholine, as well as CoA-activation happening after this step in the pathway, whereas CoA-activation happens prior to pathway commencement in the description by Pan *et al.* (2021). The resulting intermediate is subsequently converted to 5-pentadecatrienyl resorcinol by the alkylresorcinol synthases ARS1 and/or ARS2, which both are able to perform iterative condensation reactions with malonyl-CoA extender units, followed by cyclization (Cook *et al.*, 2010). Next, the O-methyl transferase SbOMT3 O-methylates the hydroxy group attached to C3 of the ring moiety to yield 5-pentadecatrienyl resorcinol-3-methyl ether. Finally, a double hydroxylation of the C4 and C6 positions is catalyzed by CYP71AM1, which yields the hydroquinone dihydrosorgoleone (Pan *et al.*, 2018). Dihydrosorgoleone is spontaneously oxidized to sorgoleone upon exudation into the rhizosphere (Weston *et al.*, 2013).

At the genomic level, the sorgoleone biosynthetic genes are not physically clustered together, but instead distributed across multiple chromosomes. *SbDES2* and *SbCYP71AM1* are localized on chromosome 4, *SbDES3* and *SbARS1* are localized on chromosome 5, *SbOMT3* is localized on chromosome 6, and *SbARS2* is localized on chromosome 8 (Okumoto *et al.*, 2025). Despite this, their expression is tightly co-regulated and root-hair specific, suggesting that metabolic channeling and coordinated transcriptional control can occur without classical gene clustering (Cook *et al.*, 2010). Although these genes are scattered across the genome, their coordinated expression in root hairs illustrates a common evolutionary strategy plants use to achieve cell-type-specific metabolic specialization. Given the ecological and agronomic significance of sorgoleone, understanding how its biosynthesis and regulation are controlled at the molecular level is critical for future engineering efforts aimed at enhancing BNI activity or weed suppression in cereal crops.

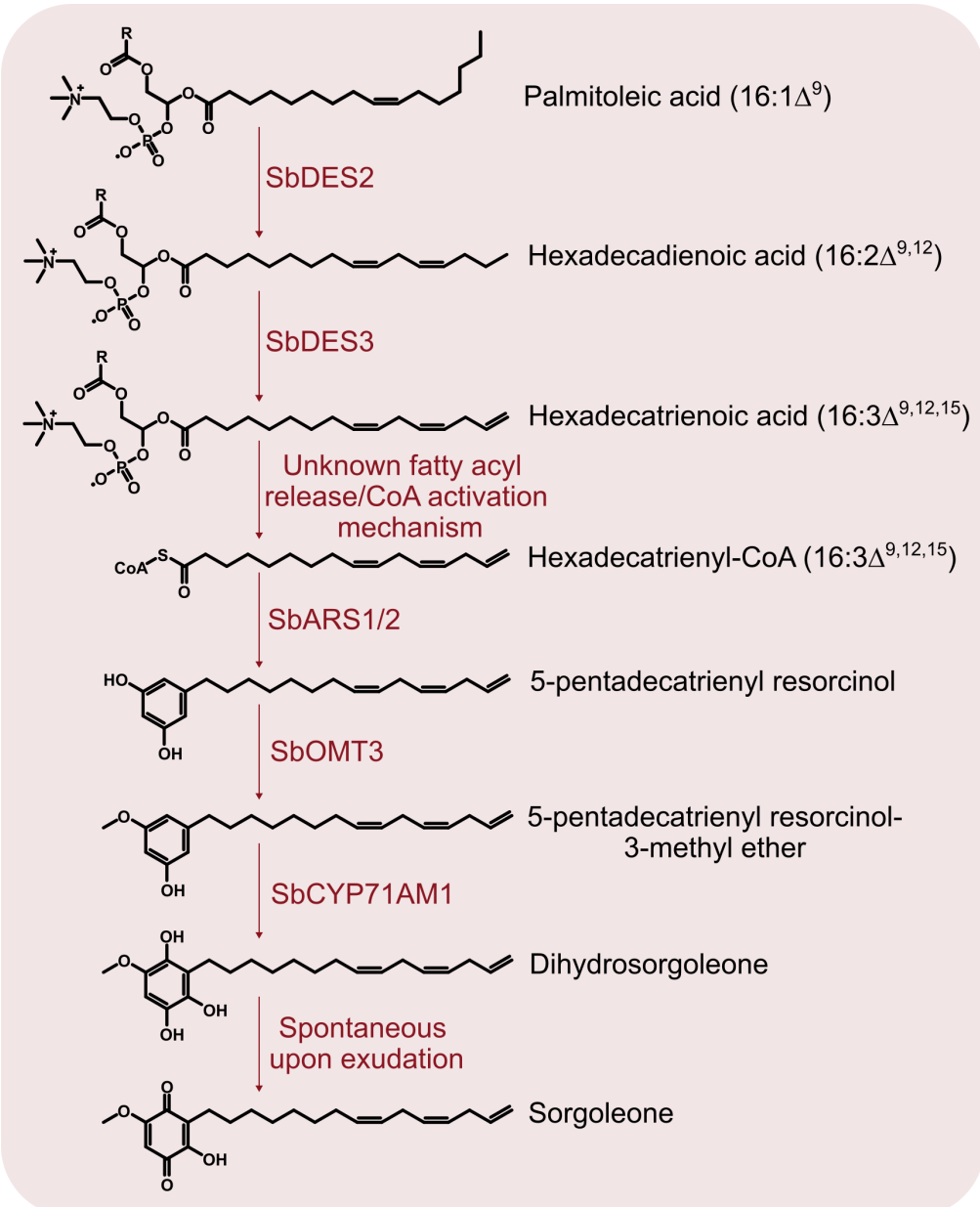


Figure 5: Proposed biosynthetic pathway for sorgoleone in sorghum as per Maharjan *et al.* (2023). R denotes second hydrocarbon chain of phosphatidylcholine.

1.4.1 Potential regulatory elements supporting sorgoleone biosynthesis

Several types of enzymes cannot function effectively on their own, but need regulation from e.g. scaffold proteins that facilitate spatial arrangement or electron carriers that provide reducing power. Cytochrome b₅ (Cytb₅) is one of such regulators, being an ER-localized heme-binding protein which shuttles electrons to proteins and enzymes (Liu, 2022). Cytb₅ proteins have been shown to provide reducing power in the biosynthesis of particular fatty acids, notably in the process of di- and tri-desaturation (Kumar *et al.*, 2012), as well as being an alternative electron donor to CYPs, which otherwise are reduced by cytochrome P450 oxidoreductases (Zhao *et al.*, 2023). While it has not been discussed before, Cytb₅ proteins could potentially be involved in providing reducing capacity to the steps involving desaturation by SbDES2 and SbDES3, as well as the oxidation step by SbCYP71AM1 in the biosynthesis of sorgoleone (Figure 5).

Another enzyme group which might also function as regulatory genes in sorgoleone biosynthesis is long-chain acyl-CoA synthetases (LACS). LACS enzymes catalyze a two step ATP-dependent reaction that preferentially converts C16+ fatty acids into CoA thioester derivatives (Zhao *et al.*, 2021). The thioester bond is highly reactive, facilitating chemical activation for metabolic enzymes such as the SbARS1/2 in the biosynthetic pathway of sorgoleone, potentially being involved in the unknown fatty acyl release/CoA activation described by (Maharjan *et al.*, 2023).

Finally, recent studies have also shown that membrane steroid binding proteins (MSBPs) from *A. thaliana* serve as scaffolding proteins that physically interact with CYPs at the ER membrane in the biosynthesis of lignin and organize them in a fashion that facilitates optimized metabolic flux (Gou *et al.*, 2018). The terminal step in the biosynthesis of sorgoleone also includes a CYP, which could need the assistance of scaffolding MSBPs. Given that MSBPs function as scaffolding proteins for ER-localized CYPs, they may similarly facilitate the organization of other ER-associated enzymes involved in sorgoleone biosynthesis, such as SbDES2, SbDES3, and SbARS1, which have been shown to form enzyme-complexes (Maharjan *et al.*, 2023).

Thesis Scope and Rationale

The scope of this thesis is to investigate secondary metabolite biosynthesis and regulation in sorghum, with a focus on compounds that mediate plant–environment interactions of ecological and agricultural importance. Two metabolites are examined as case studies: momilactone B and sorgoleone. Together these compounds exemplify two distinct but complementary aspects of plant specialized metabolism, evolutionary diversification of an allelochemical pathway and cell-type-specific regulation of a BNI.

The first case study of the thesis explores the hypothesis that momilactone B, previously reported only in the rice family and a few distantly related species, may also be produced in sorghum. Preliminary LC-MS metabolomic profiling of sorghum root hair exudates (unpublished w. Tomas Laursen) revealed a peak corresponding to the mass-to-charge ratio (m/z) of momilactone B, with a fragmentation pattern similar to what would be expected from momilactone B. Additionally, a sorghum proteomics dataset (unpublished) revealed that several enzyme orthologs to the momilactone biosynthetic enzymes in rice were highly enriched in sorghum roots. To experimentally address this observation, sorghum gene orthologs to the rice momilactone biosynthetic genes were identified and tested for functional complementation with the rice pathway in *Nicotiana benthamiana*. This approach allows functional testing of whether sorghum retains the enzymatic potential to produce momilactone diterpenoids, thereby providing insights into the evolutionary expansion and diversification of allelochemical biosynthetic pathways in the grass lineage.

The second case study of the thesis focuses on the biosynthesis and regulation of sorgoleone, the major allelochemical and BNI produced by sorghum. Previous attempts have been made by the group to reconstitute the biosynthetic pathway of sorgoleone in species *S. cerevisiae* and *Yarrowia lipolytica*, but without success. Studies have shown that all known enzymes of the sorgoleone biosynthetic pathway are highly enriched in root hairs, in accordance with the site of metabolite accumulation and secretion. The unpublished sorghum proteomics dataset also confirms enrichment of all sorgoleone biosynthetic enzymes in root hairs, and further reveals co-enrichment

of potential regulatory and supporting proteins, including a long-chain fatty-acyl-CoA synthetase (SbLACS4.1), a membrane steroid-binding protein (SbMSBP1), and an electron transporting cytochrome b₅ (SbCytb_{5.6}). These proteins are hypothesized to facilitate fatty acid activation, enzyme complex formation, or electron transfer during different steps of sorgoleone biosynthesis, potentially providing an explanation as to why efforts to reconstitute the pathway has not worked in yeast. To explore these roles, the candidate regulators were co-expressed with the pathway enzymes in *N. benthamiana*, enabling assessment of their potential influence on pathway activity and metabolite yield.

The momilactone work highlights the evolutionary relationships and potential functional conservation of diterpenoid allelochemical pathways among cereals, while the sorgoleone work investigates the spatial and molecular mechanisms controlling a well-characterized BNI pathway. Together, these studies provide complementary perspectives on sorghum's chemical ecology. One focusing on the diversification of metabolite scaffolds, the other on their cellular regulation. Ultimately, this thesis seeks to contribute to a broader understanding of bioactive root-exuded metabolites so that they eventually can be harnessed for sustainable agriculture. By attempting to elucidate the biosynthetic logic and regulatory principles underlying these natural compounds, this work positions sorghum as a powerful model for linking plant secondary metabolism with agronomic traits such as weed suppression, nitrogen use efficiency, and ecological sustainability. The findings aim to support future metabolic engineering and breeding strategies directed toward enhancing the ecological performance of cereal crops through endogenous plant chemistry, as well as efforts towards heterologous production systems.

Materials and Methods

3.1 Bioinformatic identification of sorghum orthologs

Identification and procurement was conducted by William Wajn and Tomas Laursen prior to the project start. Protein sequences of the rice momilactone biosynthetic enzymes were retrieved from the study by De La Peña and Sattely (2021) (Table 1) and used as queries for BLASTp analysis against the *Sorghum bicolor* v5.1 genome available on Phytozome. Homologous sequences with a minimum of 40% pairwise amino acid identity to the respective rice enzymes were considered potential orthologs and recorded for further evaluation. Each of the identified sorghum candidates was subsequently cross-referenced against an in-house proteomic dataset comprising sorghum root, stem, and tip samples. Proteins exhibiting preferential or root-enriched expression were prioritized as the most likely functional counterparts of the rice momilactone biosynthetic enzymes and selected for subsequent experimental testing in the *N. benthamiana* transient expression platform (Table 2). All genes were then ordered as gene fragments, codon optimized for *S. cerevisiae* and *N. benthamiana*, synthesized by Twist Bioscience (Table Appendix 2).

Momilactone – <i>Oryza sativa</i> genes						
Name	UniProt	Gene-ID	Length (AA)	Chrom. localization	Cellular localization	Tr.pep. cleavage site
OsKSL4	Q0JEZ8	Os04g0179700	842	4	plastid	56–57
OsCPS4	Q0JF02	Os04g0178300	767	4	plastid	47–48
OsCYP99A3	Q0JF01	Os04g0178400	502	4	ER	
OsCYP76M8	Q6YTF1	Os02g0569400	500	2	ER	
OsMAS	Q7FAE1	Os04g0179200	274	4	cytopl	
OsCYP76M14	Q8LJD2	Os01g0561600	524	1	ER	
OsCYP701A8	Q0DBF4	Os06g0569500	510	6	ER	

Table 1: Momilactone pathway genes in *Oryza sativa*, and their UniProt accessions, Gene-IDs, amino acid (AA) lengths, chromosome localizations, cellular localizations, and transit peptide cleavage sites.

Putative Momilactone <i>Sorghum bicolor</i> genes						
Name	UniProt	Gene-ID (Phytozome)	Length (AA)	Chrom. localiza- tion	Cellular localiza- tion	Tr.pep. cleavage site
SbKSL4	A0A1B6PN62	Sobic.006G211500	808	6	plastid	36–37
SbCYP99A3	C5YBR1	Sobic.006G010200	532	6	ER	
SbCYP76M8/14*	C5YM67	Sobic.007G152600	521	7	ER	
SbMAS	C5YFR3	Sobic.006G065300	274	6	cytopl	
SbCYP701A8	C5Z521	Sobic.010G172700	510	10	ER	

Table 2: Momilactone pathway gene orthologs in *Sorghum bicolor*, and their UniProt accessions, Gene-IDs, amino acid (AA) lengths, chromosome localizations, cellular localizations, and transit peptide cleavage sites. Gene marked with * is the top BLAST hit for both OsCYP76M8 and OsCYP76M14. Names are given based on their assumed rice counterpart, for ease of reading.

Sorgoleone biosynthetic genes and potential regulators				
Name	UniProt	Gene-ID	Length (AA)	Chrom. localiza- tion
SbDES2	A3F5L3	Sb04g029900	385	4
SbDES3	Q594P3	Sb05g000390	389	5
SbARS1	C5Y4Z2	SORBI_3005G164200	404	5
SbARS2	C5YRS1	SORBI_3008G036800	405	8
SbOMT3	A8QW53	Sb06g000820	374	6
SbCYP71AM1	C5Y125	SORBI_3004G139300	528	4
SbLACS4.1	A0A194YHC1	SORBI_3010G045500	649	10
SbMSBP1	C5WWE9	SORBI_3001G202400	223	1
Cytb _{5,6}	C5YYE5	SORBI_3009G008900	133	9

Table 3: Sorgoleone pathway genes and their UniProt accessions, Gene-IDs, amino acid (AA) lengths, and chromosome localizations.

3.2 Generation of plant expression vectors by USER cloning

Uracil-Specific Excision Reagent (USER) cloning was utilized to prepare plant expression vectors for *Agrobacterium tumefaciens* mediated transformation of *N. benthamiana*. USER cloning is a ligation-free cloning procedure based on a USER cassette that contains restriction sites for the enzymes PacI and Nt.BbvCI, which respectively open the cassette and nicks upstream from the cutting site, leaving 8 bp overhangs. DNA fragments designed with flanking sequences complementary to the vector overhangs and containing a single uracil residue adjacent to the gene insert were treated with the USER™ enzyme mix. Excision of the uracil generates complementary overhangs,

facilitating precise and seamless insertion of the fragment into the vector backbone (Nour-Eldin *et al.*, 2010). For this purpose, the shuttle vector pLIFE33 (Figure Appendix 3) was used, which contains a USER cassette downstream of an enhanced cauliflower mosaic virus 35S promoter, as well as T-DNA borders to facilitate transfer of DNA into *N. benthamiana* genomes (Amack and Antunes, 2020).

3.2.1 Preparation of vector backbone

To prepare the vector backbone, circular pLIFE33 backbone vector was double digested by restriction enzymes PacI (New England Biolabs) and Nt.BbvCI (New England Biolabs) as follows: 50 μ L reactions were made containing 10 U PacI (New England Biolabs), 10 U Nt.BbvCI (New England Biolabs), 1 μ g pLIFE33 plasmid, and 5 μ L 10x rCutSmart™ buffer (New England Biolabs). Reactions were vortexed to mix well and subsequently incubated at 37°C for 2 hours. Gel-electrophoresis was conducted on the reactions, loading 5 μ L aliquots on a 1% agarose gel running at 135 V for 25 minutes, to verify effective digestion. The reaction was cleaned using an E.Z.N.A.® cycle pure kit (Omega BIO-TEK) eluding with 30 μ L 60°C deionized water. DNA concentration was measured using a NanoDrop™ One^C Microvolume UV-Vis Spectrophotometer (Thermo Scientific).

3.2.2 Preparation of DNA inserts, and cloning reactions

Primers used in the cloning of plasmids for the momilactone B case study are found in Table Appendix 1, and the same principles were used for the sorgoleone case study for which cloning was kindly done by Kasper Hinz. Polymerase chain reactions (PCR) were performed in five 20 μ L reactions for each genetic insert. Reaction mixtures contained 2 μ L of 10 \times PCR buffer, 1 μ L dNTP mix, 1 μ L of each forward and reverse primer, 0.2 μ L PfuX7 DNA polymerase (Nørholm, 2010), 0.2 μ L template DNA, and sterile deionized water to a final volume of 20 μ L, using water as a template for negative control. PCR cycling conditions consisted of an initial denaturation at 98°C for 2 min, followed by 30 cycles of denaturation at 98°C for 30 s, annealing at 51–58°C (depending on primer pair) for 30 s, and extension at 72°C for 1 min. A final extension was performed at 72°C for 7 min, after which samples were cooled to 12°C. Amplification was confirmed by agarose gel electrophoresis, where 5 μ L of each pooled reaction was loaded on a 1% agarose gel and run at 135 V for 25 min (Figure Appendix 1). The reactions were then cleaned using an E.Z.N.A.® cycle pure kit (Omega BIO-TEK) eluding with 30 μ L

60°C sterile deionized water. USER cloning was conducted in 10 μ L reactions with 100 ng of the respective gene inserts, 30 ng of the linearized plasmid backbone, 1 U USER™ enzyme (New England Biolabs), and sterile dionized water. The reactions were incubated for 30 min at 37°C, followed by 30 min at 20°C.

Each of the resulting plasmids were then transformed into chemically competent TOP10 *Escherichia coli* cells as follows: 25 μ L aliquots of TOP10 were thawed on ice, ~100 ng of the respective plasmids were added followed by incubation for 30 min on ice. Heat shock was then applied for 45 s at 42°C in a water bath. Subsequently, 250 μ L of super optimal catabolite (SOC) broth was added to each aliquot before 5 min incubation on ice. A subsequent incubation at 37°C shaking at 500 rpm for 1 hr allowed for optimal cell recovery before plating 100 μ L on Luria-Bertani (LB) agar plates containing 100 μ g mL⁻¹ kanamycin for antibiotic selection. Plates were then incubated at 37°C for ~24 hrs.

To further check for positive transformants, colony PCR was conducted on three colonies from each transformation. To prepare the template, 3 marked colonies were gently picked with a 10 μ L pipette tip and suspended in 50 μ L sterile deionized water, and a wildtype TOP10 colony was used as a negative control. PCR reactions were prepared in 20 μ L volumes containing 10 \times PCR buffer, 2 μ L dNTPs, 1 μ L of the respective universal pLIFE33 backbone primers (Table Appendix 1), 1 μ L of the prepared template, 0.2 μ L PfuX7 DNA polymerase, and sterile deionized water. Cycle conditions started with an initial denaturation at 98°C for 5 min, followed by 35 cycles of 98°C for 30 sec, annealing at 53°C for 30 sec, and extension at 72°C for 2 min, finally finishing with a last extension at 72°C for 7 min. A gel electrophoresis was then conducted, loading 5 μ L of the respective amplifications on a 1%-agarose gel, running at 135 V for 25 min (Figure Appendix 2).

Confirmed colonies were then inoculated in 5 mL LB-broth containing 100 μ g mL⁻¹ kanamycin to grow overnight at 37°C shaking at 250 rpm. To purify plasmid DNA from the cultured colonies, an E.Z.N.A.® Plasmid DNA Mini Kit I (Omega BIO-TEK) was used according to manufacturers instructions, eluding with 30 μ L 60°C sterile deionized water. To check that no nonsense, missense, or frameshift mutations were present, samples were sent for whole-plasmid sequencing analysis performed by GENEWIZ® (Azenta Life Sciences).

3.3 Transient expression of biosynthetic pathways in *Nicotiana benthamiana*

3.3.1 Metabolic engineering steps for momilactone B precursor boost

To increase the supply of diterpene precursors in *N. benthamiana*, metabolic flux was redirected from the plastidial MEP-pathway to the cytosolic mevalonate (MEV) pathway, following the strategy of De La Peña and Sattely (2021). This rerouting was achieved by co-expressing the plasmid pTOB16 (Figure Appendix 4) harboring a geranylgeranyl pyrophosphate synthase from *Synechococcus sp.* (SpGGPPS7) and a truncated 3-hydroxy-3-methylglutaryl-CoA reductase from *S. cerevisiae* (SctHMGR), which boost the cytosolic pool of geranylgeranyl pyrophosphate (GGPP). This approach circumvents the limited transport of isoprenoid intermediates between plastids and the cytosol, enabling higher precursor availability for downstream biosynthetic enzymes. Because the engineered pathway now operates in the cytosol, enzymes that are natively plastid-localized must be truncated to remove their N-terminal transit peptides. These truncated versions (cyt-variants) ensure proper localization and compatibility with the rerouted cytosolic metabolism. Truncations of plastid localized enzymes was made in the preparation of DNA inserts (Section 3.2.2) using primers containing start codons as part of their overhang (Table Appendix 1). Transit peptide cleavage sites were identified using TargetP2.0 (Armenteros *et al.*, 2019) (Tables 1 & 2).

3.3.2 Transformation of *Agrobacterium tumefaciens*

Electrocompetent *Agrobacterium tumefaciens* GV3101 cells (Rif^R , Gent^R on Ti-helper plasmid pMP90) were transformed with plasmid DNA by electroporation. Briefly, competent cells were thawed on ice and mixed with 7.5 ng of plasmid DNA, or water as a negative control. The suspensions were transferred to pre-chilled 2 mm electroporation cuvettes (vwrTM), ensuring that the cell suspension was in contact with both electrodes and that no air bubbles were present. Electroporation was performed at 2.5 kV, 25 μF capacitance, and 200 Ω resistance. Immediately after the pulse, 1 mL yeast extract peptone (YEP) medium (without antibiotics) was added to the cuvette, and the entire mixture was transferred to a 13 mL culture tube. Each cuvette

was rinsed with an additional 1 mL of YEP medium, which was combined with the respective recovery culture. Cells were allowed to recover at 28°C for 1–2 h shaking at 150 rpm. Following recovery, 100 µL of the culture as well as a 1:10 dilution were spread on YEP-agar plates containing rifampicin (10 µg mL⁻¹) and gentamicin (25 µg mL⁻¹) for selection of the GV3101 cells, as well as kanamycin (50 µg mL⁻¹) for selection of positive transformants. Plates were incubated at 28°C for 2–3 days until colonies appeared. Plates were stored at 4°C.

3.3.3 Agroinfiltration of *Nicotiana benthamiana*

For transient expression assays, transformed *A. tumefaciens* GV3101 strains were prepared for agroinfiltration. Two to three single colonies carrying the constructs of interest were inoculated into 2 mL YEP medium supplemented with rifampicin (10 µg mL⁻¹, gentamicin (25 µg mL⁻¹), and kanamycin (50 µg mL⁻¹), and grown overnight at 28°C with shaking at 150 rpm. The following day, cultures were diluted 10× by transferring 1 mL culture into 9 mL fresh YEP medium containing only kanamycin (50 µg mL⁻¹) and supplemented with 20 µM acetosyringone to induce virulence genes. Cultures were incubated overnight at 28°C with shaking at 150 rpm.

On the day of infiltration, cells were harvested by centrifugation at 4000×*g* for 20 min at room temperature. Pellets were resuspended in infiltration buffer consisting of 10 mM MES (pH 5.6), 10 mM MgCl₂, and 200 µM acetosyringone. Optical density was determined at 600 nm (OD₆₀₀) after 1:100 dilution in water. Working suspensions were prepared by mixing the desired *A. tumefaciens* strains in equal proportions, with final ODs adjusted to 0.2 per strain. To enhance expression, a strain carrying the pLIFE33 vector with the gene silencing suppressor gene p19 (UniProt acc. P11690) was included to get a final OD₆₀₀ of 1.8 for momilactone pathway expression combinations, and 1.6 for sorgoleone pathway expression combinations (Voinnet *et al.*, 2003). A total OD₆₀₀ above 2.0 was avoided, as this caused necrosis of infiltrated leaves.

Suspensions were infiltrated into the abaxial side of leaves of 4–6 week old *N. benthamiana* plants using a 1 mL needleless syringe. To minimize variation in expression levels, leaves of similar developmental stage (typically leaf positions 4–6 from the base) were selected within each experiment. Following infiltration, plants were kept in the laboratory for several hours before being returned to the greenhouse and maintained under well-watered conditions, for 6 days.

3.4 Metabolite extraction

Metabolites for gas chromatography-mass spectrometry (GC-MS) analysis were extracted from leaf discs (6.5 mm in diameter) obtained from agroinfiltrated *N. benthamiana* leaves. Leaf material was suspended in 500 μ L 100% ethyl acetate and snap-frozen in liquid nitrogen. Samples were homogenized in 1.5 mL Eppendorf Safe-Lock[®] tubes with two 5 mm chrome beads using a Mixer Mill MM 400 (Retsch) for 2 min at 25 Hz. Homogenates were incubated at room temperature for 2 hrs with shaking at 350 rpm, followed by centrifugation at 13,000 $\times g$ for 2 min to remove debris. From each sample, 450 μ L of the supernatant was transferred to a fresh tube and dried by complete evaporation in a ScanVac centrifuge evaporator (LaboGene[™]). Dried samples from the momilactone workflow were reconstituted in 45 μ L 100% ethyl acetate containing 5 ppm 1-eicosene (internal standard) and transferred to GC-MS vials with glass inserts. Dried samples from the sorgoleone workflow were reconstituted in 22.5 μ L ethyl acetate containing 5 ppm 1-eicosene and 22.5 μ L of the derivatization agent N,O-Bis(trimethylsilyl)-trifluoroacetamide (BSTFA), followed by incubation at 70°C for 2 hrs, which then was transferred to GC-MS vials with glass inserts after cooling.

For extraction of root exudate metabolites, *S. bicolor* Btx623 seedlings were propagated by first imbibing seeds in tap water for 24 h in darkness. Subsequently, 25 seeds were placed on three layers of filter paper in culture boxes containing 20 mL tap water and incubated for 5 days at 28°C in darkness. Roots were excised from the germinated seedlings, and the basal root segments were immersed in 10 mL 10% methanol for 30 seconds each to extract root exudates. The solvent was evaporated to dryness using a ScanVac centrifuge evaporator (LaboGene[™]), after which the residue was resuspended in 100 μ L 100% ethyl acetate. This suspension was then evaporated to dryness again using the same method, followed by subsequent resuspension in 50 μ L 100% ethyl acetate containing 5 ppm of the internal standard 1-eicosene. The derivatization agent BSTFA was then added in a 1:1 ratio and incubated at 70°C for 2 hrs. Finally, the suspensions were cooled and transferred to GC-MS vials with glass inserts.

3.5 Gas chromatography - mass spectrometry

GC-MS couples a separation technique, gas chromatography, with a mass spectrometer so that individual compounds in a mixture are first separated by retention time, then each eluting compound is ionized and analyzed for its mass-to-charge (m/z) ratio. In the mass spectrometer, the molecules are bombarded by electrons, generating a molecular ion which can further fragment into charged pieces and neutral radicals, where only the charged fragments are detected. The resulting mass spectrum shows a “fingerprint” of peaks at different m/z values that correspond to specific fragment ions, and the tallest peak (base peak) reflects the most stable fragment ion formed. Because fragmentation patterns are reproducible for a given compound under defined conditions, they can be compared against reference libraries to identify unknown components in the sample (Bruice, 2014).

3.5.1 Momilactone B detection method

To analyze extraction samples from *N. benthamiana* for momilactone B and its upstream intermediates, a Shimadzu Nexis™ GC-2030 Gas Chromatogram coupled to a Shimadzu single quadrupole GCMS-QP2020 NX Gas Chromatograph-Mass Spectrometer was used. Samples were separated using an Agilent HP-5ms capillary column with a length of 30 m, thickness of $0.25\text{ }\mu\text{m}$, and a diameter of 0.25 mm, using helium as a carrier gas at a flow rate of 0.86 mL min^{-1} . A volume of $1\text{ }\mu\text{L}$ was injected to the inlet which was set to 280°C in splitless mode. Gas chromatogram oven gradient temperatures were as follows: initial temperature of 130°C for 2 min, a ramp up to 250°C with a rate of 8°C min^{-1} , followed by another ramp to 310°C at a rate of $10^\circ\text{C min}^{-1}$ and a final hold for 5 min for a total gradient time of 28 min. The mass spectrometer had an ion source temperature of 230°C and an interface temperature of 250°C . Data was collected with a scan speed of 5000 using a scan range between 50-550 m/z with a solvent cut time of 5.2 min.

3.5.2 Sorgoleone detection method

Another instrument was used for the samples from the sorgoleone *N. benthamiana* samples due to the derivatization agent BSTFA used. To analyze samples for sorgoleone and its upstream intermediates, a Shimadzu GC-2010 Gas Chromatogram coupled to a

Shimadzu single quadrupole GCMS-QP2010 Plus Gas Chromatograph-Mass Spectrometer was used. Samples were separated using an Agilent HP-5ms Ultra Inert capillary column with a length of 30 m, a thickness of $0.25 \mu\text{m}$, and a diameter of 0.25 mm, using helium as a carrier gas at a flow rate of 0.44 mL min^{-1} . A volume of $1 \mu\text{L}$ was injected to the inlet which was set to 250°C in splitless mode. Gas chromatogram oven gradient temperatures were as follows: initial temperature of 120°C for 2 min, a ramp up to 300°C with a rate of $20^\circ\text{C min}^{-1}$, and a final hold for 18 min for a total gradient time of 29 min. The mass spectrometer had an ion source temperature of 230°C and an interface temperature of 250°C . Data was collected with a scan speed of 1428 using a scan range between 40-650 m/z with a solvent cut time of 6 min.

Results

4.1 Case study 1: Momilactone B

4.1.1 Experimental setup

To evaluate whether sorghum possesses functional orthologs to the rice momilactone B biosynthetic genes, a comparative expression approach was designed. The established momilactone B pathway from rice was first transiently expressed in *N. benthamiana* as a functional reference. Individual rice genes were then systematically replaced with their putative sorghum orthologs in otherwise identical expression combinations. If the sorghum genes encoded enzymes with equivalent function, momilactone B biosynthesis would be expected to proceed normally. Conversely, lack of complementation would result in accumulation of the corresponding upstream intermediates, revealing the position and potential functional divergence of the sorghum orthologs within the pathway.

4.1.2 Expression of rice biosynthetic genes in *N. benthamiana*

Before systemic replacement with sorghum orthologs, it was necessary to know whether the experimental strategy was satisfactory. This was tested by first expressing the momilactone biosynthetic pathway from rice in *N. benthamiana*. To ensure sufficient availability of diterpene precursor for downstream biosynthesis, a precursor-boosting system was introduced using the plasmid pTOB16 in combination with the silencing suppressor P19 (also described in section 3.3.1). The pTOB16 construct encodes SctHMGR and SpGGPPS7, which enhance cytosolic GGPP [1] production (Figure Appendix 4). This system effectively increases the precursor pool available for the momilactone B pathway, compensating for the limited amount of isoprenoids in plastids. Verification of this metabolic engineering step is observed in Figure 6. Here, a large

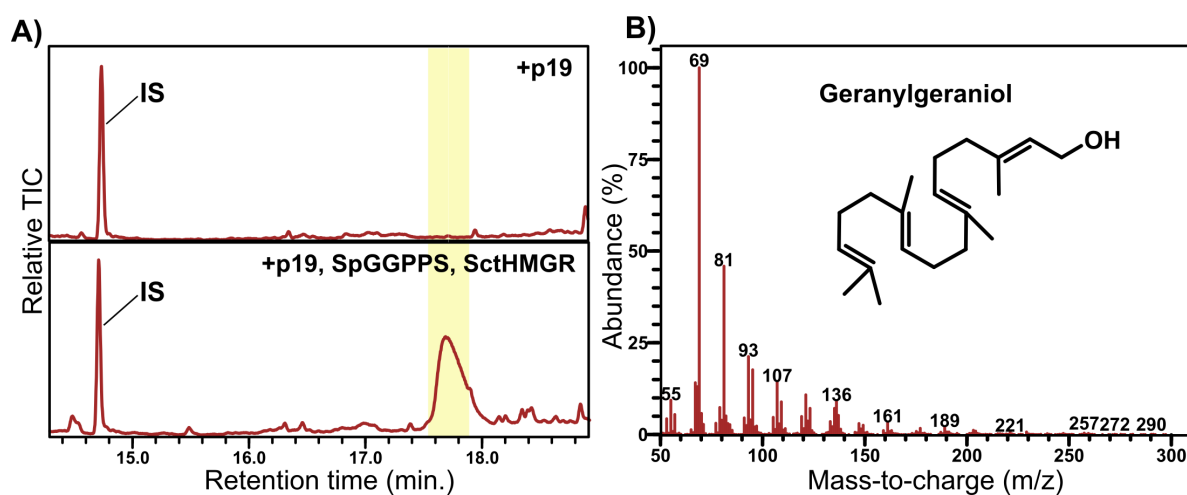


Figure 6: A) Relative total ion chromatogram (TIC) of a sample infiltrated with only *p19* (top) and a sample infiltrated with GGPP boosting genes *SpGGPPS* and *SctHMGR* (bottom), highlighting the peak representing geranylgeraniol. IS = internal standard. B) The spectrum of geranylgeraniol present in the highlighted peak from A.

peak is detectable at a retention time of 17.7 minutes in all replicates which is not detectable in the *p19* infiltrated control plants (Figure 6A). Looking at the spectral data of this peak, the molecular fingerprint corresponds to geranylgeraniol (GGOH) (Figure 6B) (Figure Appendix 5A for reference), whereas no signal corresponding to GGPP [1] was observed. This is consistent with the chemical properties of GGPP [1], which contains two phosphate groups that render the molecule highly polar and non-volatile, making it unsuitable for gas chromatographic analysis. The thermal instability of the pyrophosphate moiety likely causes hydrolysis during sample preparation or injection, resulting in the detection of the corresponding alcohol GGOH instead.

To assess the functionality of individual *A. tumefaciens* strains carrying different biosynthetic genes, *N. benthamiana* plants were infiltrated with progressively assembled gene combinations. This approach allowed evaluation of the activity of each strain in small groups and identification of pathway intermediates produced by partial gene sets. First, the truncated terpene synthases *cytOsCPS4* and *cytOsKSL4* were co-expressed together with the precursor-boosting genes. In these samples, a minor peak with a retention time of 14.4 minutes was detected (Figure 7A), displaying a spectral fingerprint corresponding to the diterpene scaffold syn-pimaradiene [3] (Figure 7B) (Figure Appendix 5C for reference).

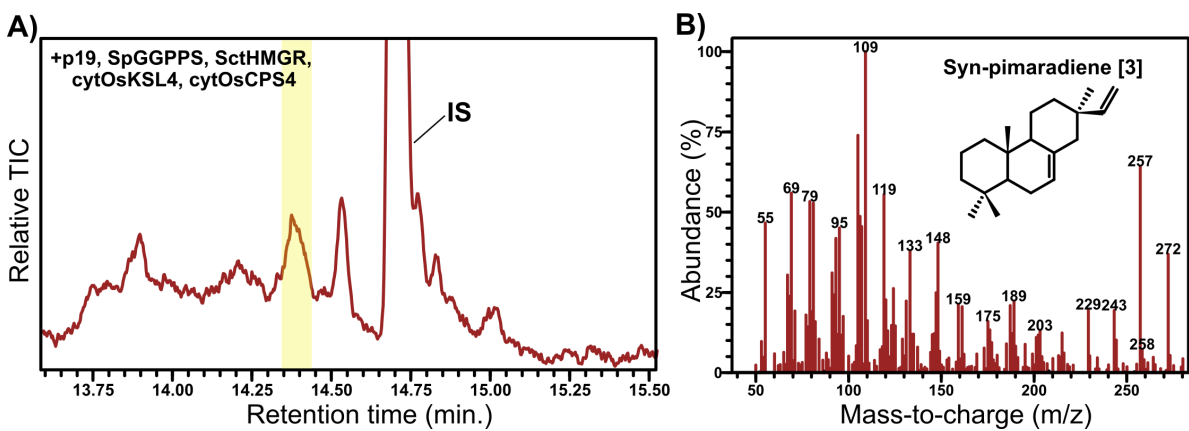


Figure 7: A) Relative total ion chromatogram (TIC) of a sample infiltrated with biosynthetic genes up to *cytOsCPS4*, showing the characteristic peak corresponding to syn-pimaradiene. IS = internal standard. B) Mass spectrum of the compound in the highlighted peak in (A), consistent with the expected fragmentation pattern of syn-pimaradiene.

Next, the momilactone-specific biosynthetic genes *OsCYP99A3*, *OsCYP76M8*, and *OsMAS* were co-expressed alongside the terpene synthases. In these samples, a distinct peak appeared at a retention time of 19.83 min (Figure 8A), with a spectral fingerprint matching the expected OsMAS product, syn-pimaradienon-19,6 β -olide [7] (Figure 8B). Additional peaks were observed at 20.65 min and 22.1 min (Figure 8A), corresponding to the downstream intermediates 20-hydroxy-syn-pimaradienon-19,6 β -olide [8] (Figure 8C) and momilactone A [9] (Figure 8D), respectively. The appearance of these compounds was unexpected, as their formation is typically catalyzed by *OsCYP76M14* and *OsCYP701A8*, which were not included in this expression batch. Their presence nonetheless suggests partial oxidation beyond the expected step and implies that the spontaneous formation of the momilactone B hemiacetal ring could also occur under these conditions. However, no signal corresponding to momilactone B was detected at the retention time of the authentic standard (Figure Appendix 8).

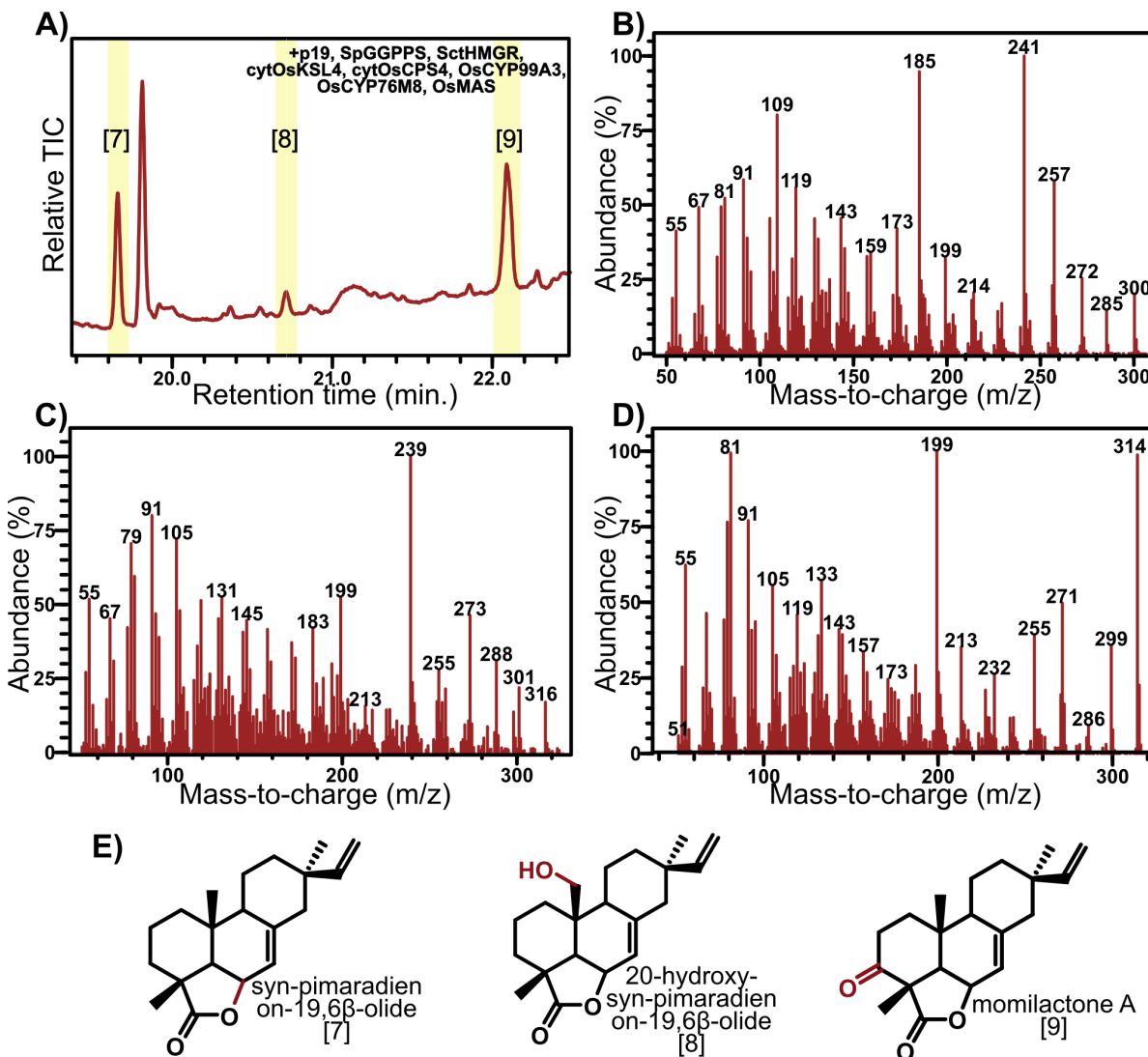


Figure 8: A) Relative total ion chromatogram (TIC) of a sample infiltrated with biosynthetic genes up to *OsMAS*, highlighting peaks corresponding to intermediates 7, 8, and 9 in momilactone B biosynthesis. B) Mass spectrum of compound 7 in (A). C) Mass spectrum of compound 8 in (A). D) Mass spectrum of compound 9 in (A). E) Names and structures of compounds 7-9.

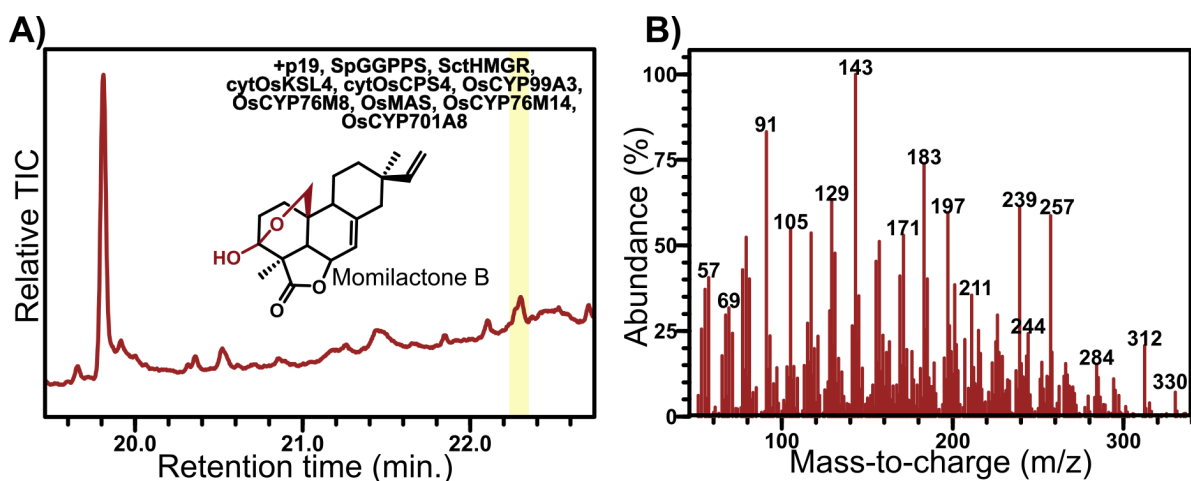


Figure 9: A) Relative total ion chromatogram (TIC) of a sample infiltrated with all biosynthetic genes in the pathway, highlighting the characteristic peak corresponding to momilactone B. B) Mass spectrum of the highlighted peak in (A), consistent with the expected fragmentation pattern of momilactone B.

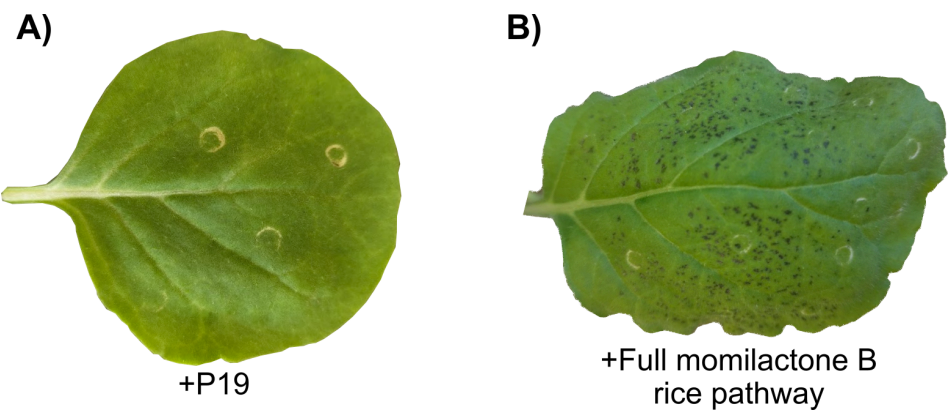


Figure 10: Phenotypes of leaves infiltrated with A) only p19 and B) with the full rice momilactone B biosynthetic pathway.

Finally, the remaining biosynthetic genes *OsCYP76M14* and *OsCYP701A8* were co-expressed with the downstream momilactone pathway. This complete transient reconstitution of the momilactone B biosynthetic pathway was expected to yield the final product, momilactone B. Indeed, a peak was detected at a retention time of 22.3 min (Figure 9A), displaying a spectral fingerprint consistent with that of momilactone B (Figure 9B). Of particular interest, infiltration of the complete rice momilactone B pathway produced a distinct leaf phenotype. In contrast to leaves infiltrated with only the p19 control at an equal OD₆₀₀, leaves expressing the full pathway developed small black spots, indicative of localized necrosis (Figure 10). This phenotype is consistent with the known phytotoxic properties of momilactone B toward certain plant species.

4.1.3 Functional complementation with sorghum ortholog genes

Using the sorghum gene candidates with the highest sequence homology to the rice momilactone B biosynthetic genes (Table 2), each ortholog was individually co-expressed with the remaining rice pathway genes to assess functional compatibility. This experiment was conducted with the expectation that successful complementation of the rice pathway with sorghum orthologs would result in detectable production of momilactone B.

Across all experiments in which individual rice genes were substituted with their sorghum orthologs, no detectable signal corresponding to momilactone B was observed in any of the samples. Similarly, the characteristic necrotic leaf phenotype associated with expression of the complete rice momilactone B pathway was absent in all sorghum-ortholog substitution infiltrations. Nevertheless, several intermediates of the pathway, including syn-copalyl hydroxide, syn-pimaradiene [3], 6 β -hydroxy-syn-pimaradiene [5], and syn-pimaradienon-19,6 β -olide [7], were successfully detected depending on the gene exchanged.

The first ortholog tested was cytSbKSL4. Samples infiltrated with this construct exhibited a prominent peak at a retention time of 17.8 minutes (Figure 11A), with a mass spectral fingerprint corresponding to syn-copalyl hydroxide (Figure 11B). The expected product of cytOsCPS4 is syn-copalyl pyrophosphate [2]; however, as with GGPP [1], compounds containing diphosphate moieties are typically not detected by GC-MS due to their thermal instability, and the hydroxylated derivative is instead observed. The strong accumulation of syn-copalyl hydroxide therefore indicates a buildup of the putative substrate for cytSbKSL4. A smaller but distinct peak was also detected at the retention time corresponding to syn-pimaradiene [3] (Figure 11A), suggesting partial turnover of syn-copalyl pyrophosphate [2] by cytSbKSL4. The spectral fingerprint of this peak aligned well with that of authentic syn-pimaradiene [3] (Figure 11C), albeit with more baseline noise than observed previously (Figure 7B). Relative quantification of peak area was done for this infiltration to visualize the spread between the three biological replicates, and the four technical replicates for each biological one (Figure 11D). While variation between biological replicates was moderate, substantial variability was observed among technical replicates derived from the same plant.

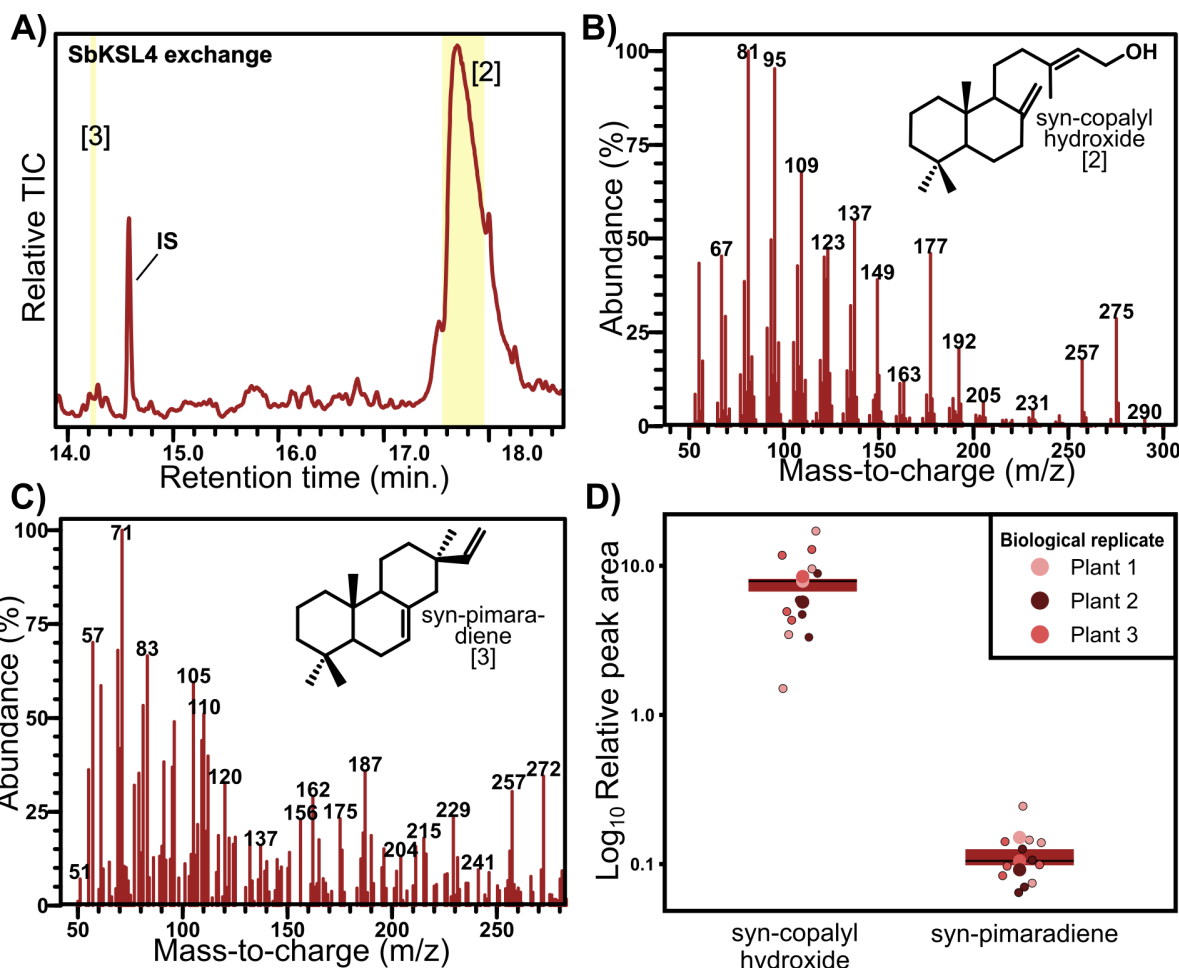


Figure 11: A) Relative total ion chromatogram (TIC) of a sample infiltrated with the momilactone B biosynthetic pathway with SbKSL4 exchanged, highlighting peaks corresponding to syn-copaly hydroxide (pyrophosphate) [2] and syn-pimaradiene [3]. B) Mass spectral fingerprint of syn-copaly hydroxide peak. C) Mass spectral fingerprint of syn-pimaradiene peak. D) Boxplot showing the peak area of syn-copaly hydroxide and syn-pimaradiene normalized to the internal standard. Variation within biological replicates was assessed across four technical replicates for each of the three independent plants ($n = 3 \times 4$).

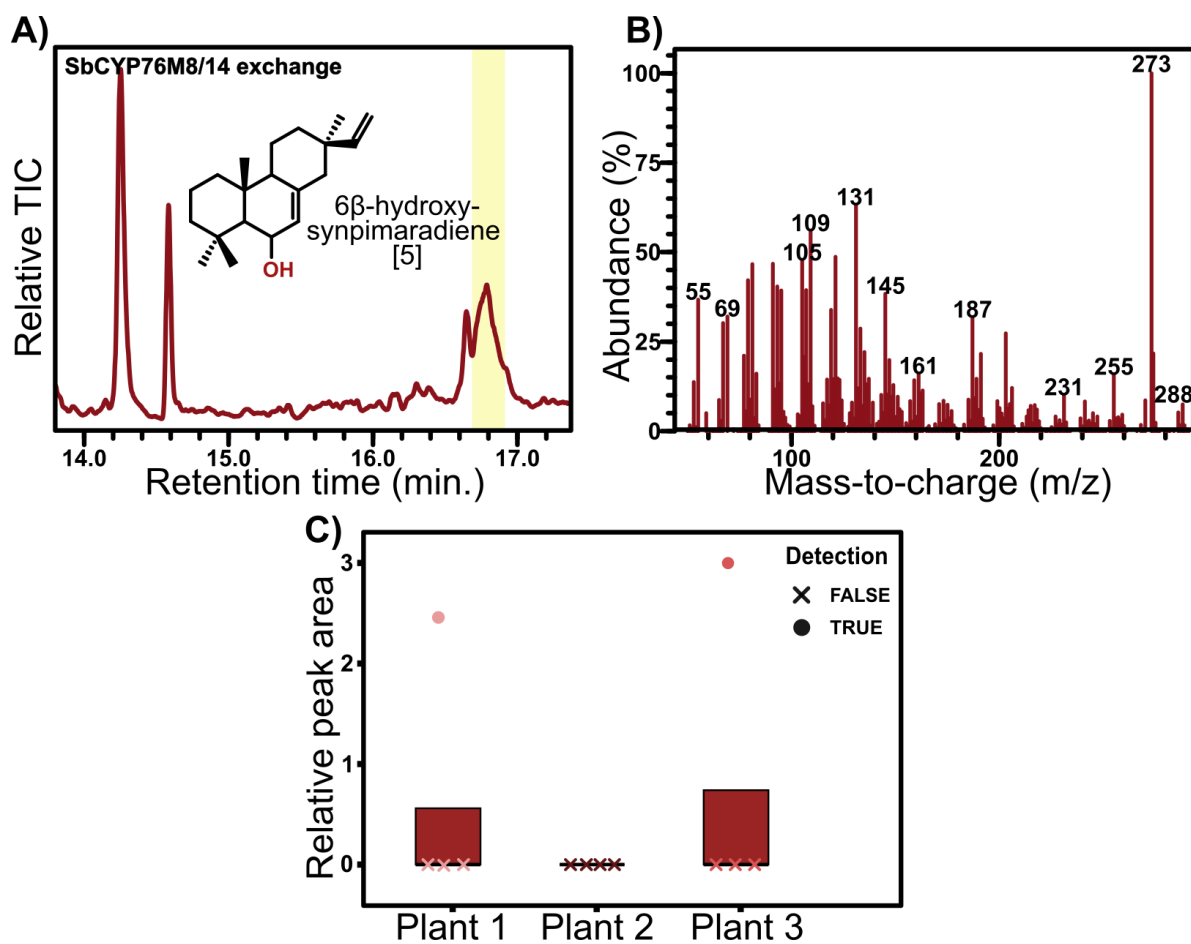


Figure 12: Relative total ion chromatogram (TIC) of a sample infiltrated with all biosynthetic genes in the pathway with SbCYP76M8/14 exchanged, highlighting the peak corresponding to 6β -hydroxy-syn-pimaradiene. B) Mass spectrum of the highlighted peak in (A). C) Box plot of the relative peak area of the three biological replicates infiltrated with this exchange, showing detection frequency of the peak in (A) within the technical replicates.

Next, the sorghum ortholog gene *SbCYP76M8/14* was tested in place of *OsCYP76M8*. Infiltrations expressing this construct produced a distinct peak at a retention time of 16.8 minutes in a subset of the samples (Figure 12A). The mass spectral fingerprint of this peak corresponded to 6β -hydroxy-syn-pimaradiene [5], the expected oxidation product of *OsCYP76M8*, which was replaced in this assay (Figure 12B). However, the compound was detected in only two of the three biological replicates, and in just one of four technical replicates per biological replicate (Figure 12C), indicating that conversion of syn-pimaradiene by *SbCYP76M8/14* occurs sporadically or with low catalytic efficiency under the tested conditions, and that endogenous *N. benthamiana* enzymes are not responsible.

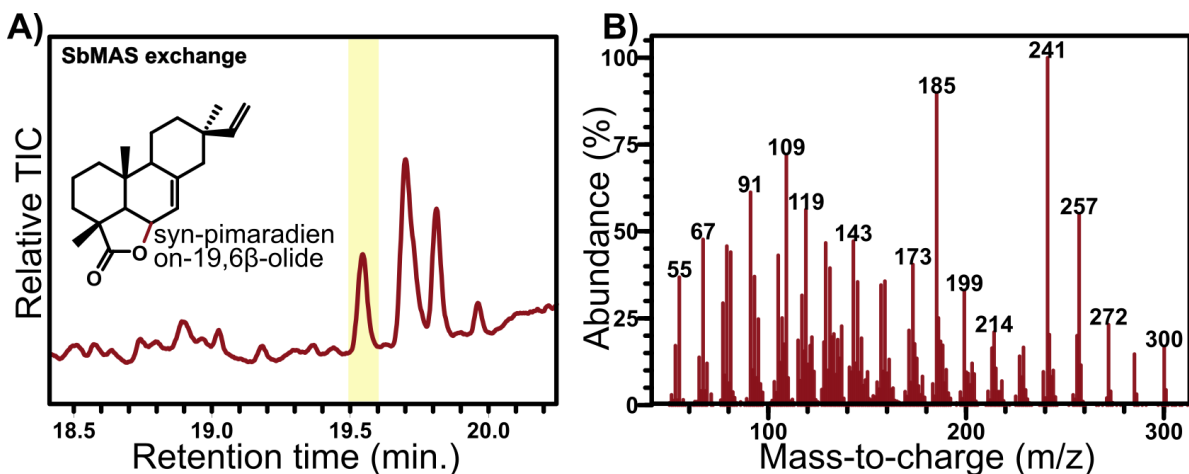


Figure 13: Relative total ion chromatogram (TIC) of a sample infiltrated with all biosynthetic genes in the pathway with SbMAS exchanged, highlighting the characteristic peak corresponding to syn-pimaradienon-19,6 β -olide [7]. B) Mass spectrum of the highlighted peak in (A).

SbCYP76M8/14 was further tested in place of OsCYP76M14, where the expected product is 20-hydroxy-syn-pimaradienon-19,6 β -olide [8]. However, no peaks corresponding to this intermediate or to momilactone B were detected in any of the samples (data not shown). Similarly, substitution of OsCYP99A3 with its putative sorghum ortholog SbCYP99A3 did not result in detectable production of syn-pimaradien-19-oic acid [4], the expected immediate product. Given that carboxylic acids are generally non-volatile and require derivatization for GC-MS detection, this compound would not be expected to appear under the analytical conditions used. Nevertheless, if SbCYP99A3 had functionally complemented the rice enzyme, downstream intermediates such as 20-hydroxy-syn-pimaradienon-19,6 β -olide [7] or momilactone B would have been observable, which was not the case in this experiment (data not shown).

Finally, the last gene ortholog, *SbMAS*, was tested in place of *OsMAS*. The expectation was that, if the sorghum enzyme could functionally complement the rice momilactone B pathway, a detectable peak corresponding to syn-pimaradienon-19,6 β -olide [7], as well as downstream intermediates, would be observed. This was indeed the case; a distinct peak with a retention time of 19.55 minutes was detected (Figure 13A), exhibiting a mass spectral fingerprint consistent with the expected intermediate (Figure 13B). The accumulation of this compound was reproducible across all biological and technical replicates of this infiltration.

4.2 Case study 2: Sorgoleone

4.2.1 Experimental setup

The experimental design of case study two followed the same overall logic as that established for case study one. Here, the biosynthetic genes of the sorgoleone pathway (Table 3) were transiently expressed in *N. benthamiana* in a series of combinatorial infiltrations, both to map the metabolic flux and intermediate accumulation along the pathway, and to assess the influence of putative regulatory or supporting factors identified from sorghum root hair proteomic data (Table 4). The first infiltration served as a negative control and contained only a single *A. tumefaciens* strain carrying *p19*. The second included *SbDES2* and *SbDES3* to examine the accumulation of the desaturated intermediate hexadecatrienoic acid (16:3Δ^{9,12,15}). The third mix added *SbARS1* and *SbARS2* to test for production of 5-pentadecatrienyl resorcinol, followed by a fourth infiltration including *SbOMT3* to evaluate formation of 5-pentadecatrienyl resorcinol-3-methyl ether. The fifth infiltration introduced the terminal enzyme *SbCYP71AM1* to determine whether expression of the complete pathway would yield dihydrosorgoleone or its oxidized form, sorgoleone.

To assess substrate flexibility at the initial desaturation steps, a sixth infiltration was conducted in which *SbDES2* and *SbDES3* were omitted, testing whether pathway completion was possible using only the endogenous 16:1Δ⁹ substrate. Finally, three additional infiltrations were performed to investigate the potential effect of co-expressing individual candidate accessory proteins *SbMSBP1*, *SbCytb_{5,6}*, and *SbLACS4.1*, together with the full biosynthetic pathway. Metabolite accumulation and pathway intermediates were subsequently analyzed by GC-MS, following the same analytical pipeline described in case study one.

A. tumefaciens strains								
Mix	1	2	3	4	5	6	7	8
1	p19							
2	p19	DES2	DES3					
3	p19	DES2	DES3	ARS1	ARS2			
4	p19	DES2	DES3	ARS1	ARS2	OMT3		
5	p19	DES2	DES3	ARS1	ARS2	OMT3	CYP71AM1	
6	p19	DES2	DES3	ARS1	ARS2	OMT3	CYP71AM1	
7	p19	DES2	DES3	ARS1	ARS2	OMT3	CYP71AM1	MSBP1
8	p19	DES2	DES3	ARS1	ARS2	OMT3	CYP71AM1	Cytb _{5,6}
9	p19	DES2	DES3	ARS1	ARS2	OMT3	CYP71AM1	LACS4.1

Table 4: Infiltration combinations of *A. tumefaciens* strains carrying different genes from the sorgoleone biosynthetic pathway.

4.2.2 Expression of sorgoleone biosynthetic genes and potential regulators in *N. benthamiana*

Since no authentic sorgoleone standard was available for GC–MS analysis, an extract of sorghum root hair metabolites was prepared (Section 3.4). This extract displayed a distinct peak at a retention time of 15.4 minutes, with a mass spectral fingerprint corresponding to dihydrosorgoleone bearing three trimethylsilyl groups, consistent with derivatization of its hydroxyl groups (Figure 14).

Analysis of samples from the various infiltration combinations revealed no detectable accumulation of the expected pathway intermediates or final products. Both derivatized and non-derivatized forms of the anticipated compounds were carefully screened for, but none were observed under the applied analytical conditions. It was further anticipated that successful expression of the full sorgoleone pathway would produce a visible leaf phenotype, as previously reported by Pan *et al.* (2021), who observed localized necrosis resulting from sorgoleone’s allelopathic activity. However, no such phenotype was detected in any of the infiltrated plants expected to produce sorgoleone analyzed in this experiment (Figure 15).

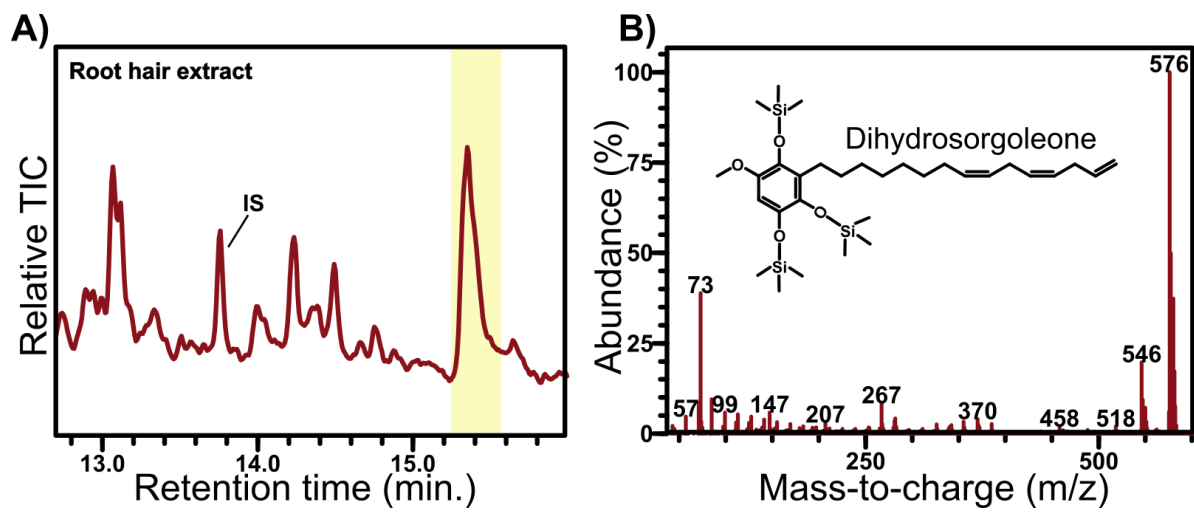


Figure 14: A) Relative total ion chromatogram (TIC) of extract from sorghum seedling root hairs, highlighting the characteristic peak corresponding to silylated dihydrosorgoleone. B) Mass spectrum of the highlighted peak in (A).

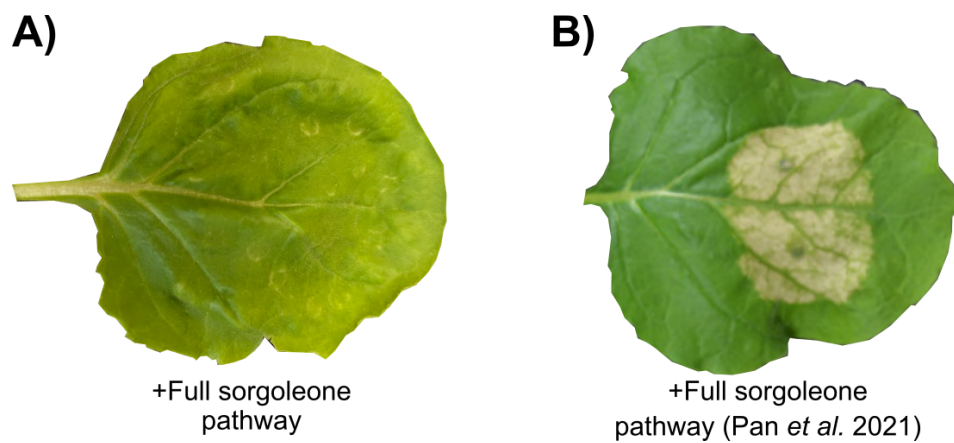


Figure 15: Leaf phenotype 6 days post infiltration of A) full biosynthetic pathway of sorgoleone in this experiment, and B) full biosynthetic pathway of sorgoleone from Pan *et al.* (2021).

Discussion

5.1 Evaluating *N. benthamiana* as a heterologous transient expression host

N. benthamiana has become one of the most widely used plant systems for transient heterologous expression of specialized metabolic pathways, including diterpenoid biosynthesis such as that of momilactone B (De La Peña and Sattely, 2021). Compared to microbial expression hosts, *N. benthamiana* provides a native plant cellular environment that supports proper mRNA processing, protein folding, and subcellular localization, which are often essential for functional reconstitution of plant enzymes. The plant also supplies endogenous metabolic precursors, co-factors, and electron transfer partners such as CYP reductases that are required for the oxidative tailoring steps of diterpene biosynthesis. Moreover, *A. tumefaciens*-mediated transient expression enables rapid combinatorial testing of pathway genes, as multiple constructs can be co-infiltrated into the same leaf to efficiently reassemble and evaluate biosynthetic routes within days (Moon *et al.*, 2020).

Despite these advantages, the same plant-specific complexity that enables successful expression can also introduce unexpected outcomes. Some samples showed the presence of downstream momilactone intermediates even when the corresponding biosynthetic enzymes were not co-expressed. For instance, the results shown in Figure 8, which contained only the first half of the rice momilactone B pathway, showed detection of compounds corresponding to the products of OsCYP701A8 and OsCYP76M14 which were not co-expressed in this assay. This suggests that endogenous enzymes in *N. benthamiana* may have complemented parts of the pathway. De La Peña and Sattely (2021) also observed production of momilactone A and B, when expressing the entire pathway without OsCYP701A8, consistent with the result observed here. They argue that expressing plant biosynthetic pathways, and in particular diterpenes that are highly modulated, will encounter endogenous enzymes to *N. benthamiana* which can functionally complement or even further metabolize intermediate scaffolds or even final products. This is also supported given the fact that plants typically encode

large CYP superfamilies, and while a total has not been reported for *N. benthamiana*, other plants such as *A. thaliana* has 244 CYPs (Bak *et al.*, 2011), *O. sativa* has 355 CYPs (Wei and Chen, 2018), and the fellow nightshade *Solanum lycopersicum* has 233 CYPs (Vasav and Barvkar, 2019). These numbers stand in stark contrast to the only three CYPs present in the genome of *S. cerevisiae* (Nelson, 2018), which also was considered as a host for this experiment. Using *S. cerevisiae* as a heterologous expression host would reduce interference from endogenous enzymes, as well as offer more consistency in results due to stable integration, in contrast to the transient expression in *N. benthamiana* (Gülck *et al.*, 2020). Together, this comparison illustrates how plant and microbial hosts offer complementary advantages. A combined strategy using both systems could therefore balance biological relevance with mechanistic clarity in future pathway reconstructions.

While some CYPs act with strict substrate specificity, many have been shown to possess degrees of promiscuity, capable of accepting multiple related substrates or catalyzing oxidations at several different positions of a substrate (Werck-Reichhart, 2023). This promiscuity provides an evolutionary mechanism for diversification, where gene duplication and subsequent neofunctionalization give rise to families of CYPs with overlapping yet distinct catalytic functions. In diterpene biosynthesis, such behavior is especially pronounced. For instance, CYP76 and CYP71 family members are frequently recruited across plant lineages to oxidize labdane-type backbones at different sites, generating a wide range of diterpenoid products (Bathe and Tissier, 2019). Notably, OsCYP76M8 exemplifies this catalytic flexibility, as it hydroxylates several distinct diterpene skeletons at alternative carbon positions depending on the available substrate, being syn-pimaradiene in the case of momilactone B biosynthesis (Werck-Reichhart, 2023). This promiscuity also raises the possibility that the heterologously expressed CYPs in this experiment may themselves display catalytic flexibility, acting on unintended substrates or producing alternative oxidation products. Such behavior may contribute to the formation of unexpected intermediates or side products when expressing diterpene pathways in *N. benthamiana*, where both endogenous and introduced CYPs can recognize and act on shared intermediates. This cross-reactivity could also explain why momilactone B was not detectable in the SbMAS exchange, which was unexpected since it otherwise appeared to complement the rice pathway (Figure 13). In hindsight, it would have been advantageous to include control infiltrations in which individual rice biosynthetic genes were omitted, mirroring the setup used for the sorghum ortholog exchange assays, but without substituting the missing gene. Such combinations would have provided a clearer indication at each step of the pathway as to whether background activity from endogenous *N. benthamiana* enzymes

or promiscuous activity from the overexpressed rice enzymes could complement the missing function.

Some questions also arise about *N. benthamiana* regarding reproducibility when looking at the results from Figure 12. Here only two out of three biological replicates, and only in the respective one of four technical replicates from each of these, produced a peak corresponding to the anticipated product. Although the production of the SbCYP76M8 product was not consistent, the presence of the compound in two independent biological replicates suggests that production may be sporadic, only occur under specific physiological conditions, or plainly due to bad expression, warranting further investigation. Looking at Figure 11D, specifically at the mean production of syn-copalyl pyrophosphate/hydroxide, a remarkable variation in peak-area is observable within technical replicates, with the differences in peak areas ranging up to 11-fold between two technical replicates from plant 1. This underscores the variation that is possible when transiently expressing multiple genes at the same time in *N. benthamiana*. Bashandy *et al.* (2015) made a comprehensive hierarchical experiment designed to map the different sources of variation in transient expression experiments in *N. benthamiana* using a luciferase reporter. They found that the largest sources of variation for infiltrations conducted on plants with uniform morphology and growth parameters was within infiltrated leaves themselves, responsible for 66% of variance observed, and within individual leaves sampled (33%). (Bashandy *et al.*, 2015) could not pinpoint the exact mechanisms underlying the variability within these, but attributed it to the sum of many small errors or differences that could accumulate at different sites of expression. These findings align well with the variability observed in this experiment, suggesting that much of the inconsistency observed in metabolite accumulation likely arises from local differences in infiltration efficiency, transient gene expression, or leaf physiology rather than from the biosynthetic pathway itself. This inherent variability highlights the importance of experimental replication and careful interpretation when evaluating pathway functionality in *N. benthamiana* as a heterologous host. The addition of more biological replicates could have resulted in higher detection frequency of the expected peak for SbCYP76M8, and therefore more statistical power towards a conclusion that it would be able to functionally complement the rice momilactone B pathway. Taken together, these observations emphasize that while *N. benthamiana* remains a powerful system for rapid pathway testing and functional screening of plant biosynthetic pathways, its inherent variability and enzymatic background make it less suited for precise quantitative studies or conclusive enzyme validation.

5.2 Evolution of momilactone biosynthetic gene clusters with respect to sorghum

The results from the ortholog exchange assays showed that several of the assayed sorghum genes exhibited partial functional compatibility with their rice counterparts, with very low detection of the SbKSL4 product (Figure 11), sporadic activity for Sb-CYP76M8/14 (Figure 12, and most notably SbMAS, which consistently complemented the rice pathway (Figure 13). This shows that some sorghum orthologs retain ancestral catalytic functionality with respect to momilactone B production. Additionally, a momilactone B standard was compared to the original peak detected in sorghum root exudate that was hypothesized to be momilactone B while the exchange assays were being conducted, and it was determined that these had different retention times (data not shown). These findings suggest that although sorghum shares homologous genes with the rice momilactone B pathway, it likely does not produce momilactone B itself. This observation fits within a broader evolutionary framework that explains how momilactone biosynthetic gene clusters arose and diversified among grasses. There is evidence for the biosynthesis of momilactones in nine grass family (*Poaceae*) plants, of which eight of them, including rice, belong to the *Oryzoideae* subfamily of the BOP grass clade, and one, *E. crus-galli*, belongs to the *Panicoideae* subfamily of the PACMAD grass clade (Mao *et al.*, 2020). Recent genomic studies have revealed that these gene clusters in grasses likely originated through lateral gene transfer (LGT) events rather than vertically through offspring (Wu *et al.*, 2022). Specifically, evidence suggests that an ancestral momilactone biosynthetic gene cluster first formed in *Triticeae* species (wheat and barley relatives), and was transferred into the PACMAD clade of grasses which includes sorghum, via LGT. A subsequent transfer event then brought a modified version of the cluster into the *Oryzoideae*, where it became the cluster found in rice today (Wu *et al.*, 2022). These transfers allowed distant grass species to rapidly acquire the ability to produce momilactones.

Interestingly, remnants of the momilactone biosynthetic gene cluster are still present in several grasses that have not been shown to produce momilactones. Sorghum is a notable example, where SbKSL4, SbCYP99A3, and SbMAS remain physically clustered on chromosome 6 (Table 2), while rice has the same with an addition of OsCPS4. Mao *et al.* (2020) demonstrated that only *Poaceae* species containing this complete four-gene cluster comprising CPS4, KSL4, CYP99A3, and MAS homologs, arranged in a similar genomic configuration to that of rice, are capable of producing

momilactone B. While some of the sorghum orthologs showed partial functional compatibility in heterologous assays, most notably SbMAS, the wider results suggest that these enzymes are unlikely to participate in the biosynthesis of momilactone B specifically in sorghum. Instead, their residual activity may reflect conservation of ancestral catalytic properties, supporting the idea that these genes have been retained because they contribute to related or derived metabolic processes.

The persistence of such clusters in species that no longer synthesize momilactones raises intriguing questions about the evolutionary forces driving their maintenance. One plausible explanation is that the cluster, or parts of it, as well as the CYPs that were not clustered, continues to provide adaptive value by being co-opted into other branches of specialized metabolism or defense. This fits well within the evolutionary principle 'use it or lose it'. Retention of these genes may therefore reflect their broader functional utility in plant stress responses or chemical defense, even if the original biosynthetic role has been lost. Kitaoka *et al.* (2021) supports this by highlighting that because of the mostly vertical evolution of plants, biosynthetic gene clusters often need to evolve interdependently with other biosynthetic gene clusters that harbor enzymes with complementary or catalytically promiscuous functions, such as the momilactone B cluster. In this context, the sorghum orthologs may represent evolutionary relics that have been repurposed, providing metabolic flexibility and the potential for future neofunctionalization.

Collectively, these findings suggest that while sorghum does not synthesize momilactone B, the maintenance and partial functionality of its orthologous genes to those of the rice pathway point to a wider role in the diversification and plasticity of plant secondary metabolism. This conservation supports the idea that gene clusters can persist and evolve new functions, providing plants with a versatile toolkit for responding to environmental challenges. The orthologs that showed degrees of functional complementation are likely still involved in production of similar labdane-related diterpenoids, which could also have the same mass-to-charge ratio and similar fragmentation as momilactone B, potentially explaining the peak originally believed to be momilactone B in sorghum root exudate. To unambiguously identify the metabolite responsible for this signal, further structural elucidation would be required, for example through high-performance liquid chromatography purification followed by NMR spectroscopy as done by e.g. Brkljača and Urban (2015).

5.3 Experimental setup of sorgoleone pathway expression

Following the successful reconstitution of the momilactone B biosynthetic pathway and partial complementation with sorghum orthologs, the same heterologous expression system was applied to test the putative regulation of the sorgoleone biosynthetic genes in *N. benthamiana*. Since the expression of the momilactone B biosynthetic genes and orthologs was successful, it was hypothesized that the same method could be used for expressing the sorgoleone biosynthetic pathway in *N. benthamiana*, a host that has already proven suitable for expressing this pathway in earlier work by Pan *et al.* (2021). However, after diligent analysis of the resulting GC-MS data, neither pathway intermediates nor peaks corresponding to the dihydrosorgoleone peak identified in root exudate (Figure 14) were observed in any of the samples analyzed. The expected leaf phenotype of the plants infiltrated with the entire biosynthetic pathway, pictured in Figure 15B, was not observed either.

The absence of detectable metabolites together with the lack of the characteristic necrotic phenotype indicates that the sorgoleone pathway was not functionally expressed in the infiltrated *N. benthamiana* leaves. This likely reflects fundamental faults in the expression assay, and exposes some limitations of the experimental setup. The first thing to do would be to conduct a colony PCR to check if transformed *A. tumefaciens* colonies were indeed carrying the respective binary vectors, which was otherwise thought to be unnecessary due to the combination of antibiotics used on the culture plates. However, if the plasmids were indeed present, the successful growth of *A. tumefaciens* strains on selective antibiotics only confirms the presence of the pLIFE33 vector with gene insert, but does not guarantee that the introduced genes were transcribed or translated *in planta*. Post-transcriptional gene silencing is a well-known complication when multiple constructs driven by identical regulatory elements, such as the enhanced 35S promoter used for co-expression of all sorgoleone genes in the same tissue. The repetitive promoter sequences can enhance post-transcriptional gene silencing that effectively suppresses transgene expression, resulting in no detectable enzyme activity despite successful infiltration (Chung *et al.*, 2005; Peremarti *et al.*, 2010). However, Grützner *et al.* (2024) successfully co-expressed up to 13 genes under the same promoter in *N. benthamiana* without experiencing this, which is in concordance with the up to 8 genes in the momilactone case-study, where no gene silencing occurred either.

Nevertheless, comparison with the successful sorgoleone expression reported by Pan *et al.* (2021) reveals several key methodological differences that may explain the discrepancy observed in the results presented here and in their study. They assembled all biosynthetic genes into a single vector with diversified promoters and terminators to reduce post-transcriptional gene silencing, and critically verified transgene expression through RT-qPCR and RNA-sequencing analysis. Their approach ensured coordinated delivery of all pathway components to the same cells and allowed for optimized enzyme stoichiometry factors that may be compromised when relying on separate *A. tumefaciens* strains with potentially variable infiltration efficiency and expression levels. Adopting such an approach could have provided insight into whether the biosynthetic genes were actively transcribed, and if they were subject to silencing. Another approach could have been to tag the enzymes with green fluorescent protein (GFP) or histidine (his) repeats. The first approach could mimic Sáiz-Bonilla *et al.* (2022) who implemented a GFP-tag to verify expression and expected localization of their protein of interest in *N. benthamiana* using confocal microscopy. The second approach can be illustrated by Soni *et al.* (2022) who used 6xhis-tags to verify that their protein of interest was being adequately expressed and translated by making Western-blots using anti-his antibodies.

From an analytical perspective, future work should include a systematic validation of intermediate formation through sequential expression of the individual biosynthetic enzymes, beginning with the desaturases (SbDES2 and SbDES3). Each step should be monitored by GC-MS against authentic standards, where available, to verify product identity and ensure that each enzymatic reaction proceeds as expected. This approach would mirror the analytical workflow of Pan *et al.* (2007), who identified and functionally characterized the sorgoleone biosynthesis desaturases responsible for producing 16: Δ 2 and 16: Δ 3 fatty acids through methyl esterification and comparison to verified fatty-acid standards. Establishing such analytical checkpoints would confirm intermediate formation even in cases where the complete pathway fails to produce the final compound.

Implementing these verification strategies, alongside optimization of promoter diversity and construct design, would not only confirm transgene expression, but also help determine whether the observed lack of product formation in this study reflects transcriptional silencing, translational failure, or the fundamental transformation or cloning steps in the beginning of the experimental workflow, as well as ensuring the validation of all steps in the pathway.

Conclusion

This thesis explored two facets of sorghum specialized metabolism: the evolutionary diversification of diterpenoid allelochemicals exemplified by momilactone B, and the regulation of lipid-derived alkylresorcinols exemplified by sorgoleone. Transient expression of rice momilactone B biosynthetic genes in *N. benthamiana* successfully reconstructed the pathway and demonstrated that selected sorghum orthologs can functionally complement individual steps, supporting partial conservation of diterpenoid biosynthetic capability in sorghum. However, the absence of full pathway reconstitution and variability among replicates emphasize the complexity of enzyme compatibility and the influence of the host metabolic background.

The sorgoleone experiment, in contrast, revealed no detectable metabolite formation, suggesting fundamental flaws in the experimental design. The absence of metabolite production could be tied to either absence of genes in *A. tumefaciens*, post-transcriptional gene silencing, or enzymatic shortcomings. The lack of the characteristic necrotic phenotype and of pathway products underscores the importance of verifying transgene expression and optimizing construct design, particularly for multigene assemblies, even if otherwise successful in other pathway reconstructions.

Overall, the findings underline *N. benthamiana*'s suitability for qualitative testing of individual enzyme functions, but also its limitations for reconstructing entire multistep pathways from other plants. Despite the experimental challenges, the work provides a framework for probing biosynthetic evolution, testing ortholog functionality, and identifying the molecular constraints that shape plant chemical diversity.

Perspectives

The continuing pursuit to understand plant secondary metabolism is not merely an academic exercise in cataloging chemical diversity, but rather represents a frontier for reimagining how agriculture and biotechnology can align through innovation. The pathways underlying allelochemicals and BNIs exemplify this potential. Both classes of metabolites reveal how plants have evolved these intricate chemical strategies to regulate nutrient fluxes through interactions with microbial communities and plants that compete for nutrients in the rhizosphere. Deciphering of these strategies at the molecular level will be essential to translate nature's solutions into scalable, sustainable technologies, which lies at the heart of what biotechnology is.

Modern agriculture still relies heavily on synthetic inputs that disrupt natural nutrient cycles. Harnessing the biosynthetic potential of plants provides an alternative paradigm. One where biological systems instead of synthetic chemistry mediate soil processes and ecosystem balance. Yet, realizing this vision demands a deep understanding of the metabolic logic that governs pathway organization, enzyme specificity, cellular compartmentalization, and regulatory mechanisms involved. The fact that many BNI and allelopathic compound pathways remain completely unknown or only partially resolved underscores both the biochemical complexity and the transformative opportunity that lies ahead.

By integrating genomics, metabolomics, and synthetic biology, future research can move from pathway reconstruction to rational design, engineering crops themselves that express optimized versions of these naturally evolved biochemical traits. Once validated, these optimized traits could be introduced into elite crop varieties through introgression breeding programs or genome editing, forming the basis for large-scale, field-level deployment. Alternatively, efforts towards precision fermentation of these compounds could also make them widely available and applicable in optimal combinations suitable for different environments. Pilot-scale fermentation and downstream purification trials could be expanded into bioreactor production platforms to meet agricultural demand. Such efforts could sustainably stabilize nitrogen in soils, reduce fertilizer dependency, suppress weeds, and reduce greenhouse gas emissions. Beyond

agronomy, these discoveries will expand our general understanding of metabolic evolution, revealing how plants convert simple precursors into multifunctional compounds that serve both ecological and physiological functions. Further studies should not only continue to elucidate the detailed biosynthetic mechanisms of these compounds but also adopt a holistic perspective on their function and application, considering their interactions with both target and non-target organisms, as well as the environmental and physiological factors that influence their activity and production.

Ultimately, advancing plant secondary metabolism research is about learning to work with the chemical intelligence of nature. The allelopathic and BNI systems studied here offer a glimpse of what becomes possible when biotechnology takes its cues from evolution itself, being sustainable, self-regulating biosolutions that channel the force of nature toward the grand challenge of building resilient agricultural ecosystems.

Bibliography

- Alquézar, Berta, Haroldo Xavier Linhares Volpe, Rodrigo Facchini Magnani, Marcelo Pedreira De Miranda, Mateus Almeida Santos, Nelson Arno Wulff, Jose Mauricio Simões Bento, José Roberto Postali Parra, Harro Bouwmeester, and Leandro Peña (Dec. 2017). „ β -caryophyllene emitted from a transgenic *Arabidopsis* or chemical dispenser repels *Diaphorina citri*, vector of *Candidatus Liberibacters*“. In: *Scientific Reports* 7.1.
- Amack, Stephanie C. and Mauricio S. Antunes (Dec. 2020). „CaMV35S promoter – A plant biology and biotechnology workhorse in the era of synthetic biology“. In: *Current Plant Biology* 24.100179.
- Aminpanah, H, A Sorooshzadeh, E Zand, and A Moumeni (2013). „Competitiveness of Rice (*Oryza sativa* L.) Cultivars against Barnyardgrass (*Echinochloa crus-galli* (L.) P. Beauv.) in Lowland Rice Fields“. In: *Thai Journal of Agricultural Science* 46.4, pp. 209–217.
- Arend, Kristin K., Dmitry Beletsky, Joseph V. Depinto, Stuart A. Ludsin, James J. Roberts, Daniel K. Rucinski, Donald Scavia, David J. Schwab, and Tomas O. Höök (Feb. 2011). „Seasonal and interannual effects of hypoxia on fish habitat quality in central Lake Erie“. In: *Freshwater Biology* 56.2, pp. 366–383.
- Armenteros, Jose Juan Almagro, Marco Salvatore, Olof Emanuelsson, Ole Winther, Gunnar Von Heijne, Arne Elofsson, and Henrik Nielsen (2019). „Detecting sequence signals in targeting peptides using deep learning“. In: *Life Science Alliance* 2.5.
- Bajwa, Ali Ahsan (2014). „Sustainable weed management in conservation agriculture“. In: *Crop Protection* 65, pp. 105–113.
- Bak, Søren, Fred Beisson, Gerard Bishop, Björn Hamberger, René Höfer, Suzanne Paquette, and Danièle Werck-Reichhart (Jan. 2011). „Cytochromes P450“. In: *The Arabidopsis Book*. Vol. 9. American Society of Plant Biologists, e0144.
- Bashandy, Hany, Salla Jalkanen, and Teemu H. Teeri (Oct. 2015). „Within leaf variation is the largest source of variation in agroinfiltration of *Nicotiana benthamiana*“. In: *Plant Methods* 11.47.
- Bathe, Ulschan and Alain Tissier (May 2019). „Cytochrome P450 enzymes: A driving force of plant diterpene diversity“. In: *Phytochemistry* 161, pp. 149–162.

- Beeckman, Fabian, Hans Motte, and Tom Beeckman (Apr. 2018). „Nitrification in agricultural soils: impact, actors and mitigation“. In: *Current Opinion in Biotechnology* 50, pp. 166–173.
- Belz, Regina G., Karl Hurle, and Stephen O. Duke (Apr. 2005). „Dose-Response—A Challenge for Allelopathy?“ In: *Nonlinearity in Biology, Toxicology, Medicine* 3.2.
- Botella, César, Juliette Jouhet, and Maryse A. Block (Jan. 2017). „Importance of phosphatidylcholine on the chloroplast surface“. In: *Progress in Lipid Research* 65, pp. 12–23.
- Bouhaouel, Imen, Aurélie Gfeller, Marie Laure Fauconnier, Salah Rezgui, Hajar Slim Amara, and Patrick du Jardin (June 2015). „Allelopathic and autotoxicity effects of barley (*Hordeum vulgare* L. ssp. *vulgare*) root exudates“. In: *BioControl* 60.3, pp. 425–436.
- Brklača, Robert and Sylvia Urban (July 2015). „HPLC-NMR and HPLC-MS Profiling and Bioassay-Guided Identification of Secondary Metabolites from the Australian Plant *Haemodorum spicatum*“. In: *Journal of Natural Products* 78.7, pp. 1486–1494.
- Bruice, Paula Yurkanis (2014). „14: Mass Spectrometry, Infrared Spectroscopy, and Ultraviolet/Visible Spectroscopy“. In: *Organic Chemistry*. Ed. by Adam Jaworski. 7th ed. Upper Saddle River, NJ, USA: Pearson Education, pp. 595–611.
- Castro Marcato, Ana Claudia de, Cleiton Pereira de Souza, and Carmem Silvia Fontanetti (Mar. 2017). „Herbicide 2,4-D: A Review of Toxicity on Non-Target Organisms“. In: *Water, Air, and Soil Pollution* 228.3.
- Chung, Sang-Min, Ellen L. Frankman, and Tzvi Tzfira (Aug. 2005). „A versatile vector system for multiple gene expression in plants“. In: *Trends in Plant Science* 10.8, pp. 357–361.
- Cook, Daniel, Agnes M. Rimando, Thomas E. Clemente, et al. (2010). „Alkylresorcinol synthases expressed in Sorghum bicolor root hairs play an essential role in the biosynthesis of the allelopathic benzoquinone sorgoleone“. In: *Plant Cell* 22.3, pp. 867–887.
- Curl, Cynthia L., Meredith Spivak, Rachel Phinney, and Luke Montrose (Mar. 2020). „Synthetic Pesticides and Health in Vulnerable Populations: Agricultural Workers“. In: *Current environmental health reports* 7.1, pp. 13–29.
- De La Peña, Ricardo and Elizabeth S. Sattely (Feb. 2021). „Rerouting plant terpene biosynthesis enables momilactone pathway elucidation“. In: *Nature Chemical Biology* 17.2, pp. 205–212.
- Dykes, Linda, Larry M. Seitz, William L. Rooney, and Lloyd W. Rooney (Sept. 2009). „Flavonoid composition of red sorghum genotypes“. In: *Food Chemistry* 116.1, pp. 313–317.

- Egenolf, Konrad, Jochen Schöne, Jürgen Conrad, Christina Braunberger, Uwe Beifuß, Jacobo Arango, and Frank Rasche (2023). „Root exudate fingerprint of Brachiaria humidicola reveals vanillin as a novel and effective nitrification inhibitor“. In: *Frontiers in Molecular Biosciences* 10.
- European Commission (Sept. 2025). „Pesticide reduction targets - Progress“. In: https://food.ec.europa.eu/plants/pesticides/sustainable-use-pesticides/pesticide-reduction-targets-progress_en Accessed: 16/09/2025.
- Ghatak, Arindam, Alexandros E. Kanellopoulos, Cristina López-Hidalgo, et al. (2025). „Natural variation of the wheat root exudate metabolome and its influence on biological nitrification inhibition activity“. In: *Plant Biotechnology Journal*, pp. 1–18.
- Glibert, Patricia M., Sybil Seitzinger, Cynthia A. Heil, Joann M. Burkholder, Matthew W. Parrow, Louis A. Codispoti, and Vince Kelly (2005). „The Role of Eutrophication in the Global Proliferation of Harmful Algal Blooms“. In: *Oceanography* 18.2, pp. 198–209.
- Gonzalez, Veronica Miranda, Janet Kazimir, Chandrashekhar Nimal, Leslie A Weston, and G M Cheniae (1997). „Inhibition of a Photosystem II Electron Transfer Reaction by the Natural Product Sorgoleone“. In: *Journal of Agricultural and Food Chemistry* 45.4.
- Gou, Mingyue, Xiuzhi Ran, Dwight W. Martin, and Chang Jun Liu (May 2018). „The scaffold proteins of lignin biosynthetic cytochrome P450 enzymes“. In: *Nature Plants* 4.5, pp. 299–310.
- Grützner, Ramona, Kristin König, Claudia Horn, Carola Engler, Annegret Laub, Thomas Vogt, and Sylvestre Marillonnet (May 2024). „A transient expression tool box for anthocyanin biosynthesis in Nicotiana benthamiana“. In: *Plant Biotechnology Journal* 22.5, pp. 1238–1250.
- Gülck, Thies, J. K. Booth, Carvalho, B. Khakimov, C. Crocoll, M. S. Motawia, B. L. Møller, J. Bohlmann, and N. J. Gallage (Oct. 2020). „Synthetic Biology of Cannabinoids and Cannabinoid Glucosides in Nicotiana benthamiana and Saccharomyces cerevisiae“. In: *Journal of Natural Products* 83.10, pp. 2877–2893.
- Halkier, Barbara Ann and Birger Lindberg Møller (1989). „Biosynthesis of the Cyanogenic Glucoside Dhurrin in Seedlings of Sorghum bicolor (L.) Moench and Partial Purification of the Enzyme System Involved“. In: *Plant Physiol* 90.4, pp. 1552–1559.
- Jahan, Tanzim, Md Nurul Huda, Kaixuan Zhang, et al. (Mar. 2025). *Plant secondary metabolites against biotic stresses for sustainable crop protection*.
- Kalinger, Rebecca S., Ian P. Pulsifer, Shelley R. Hepworth, and Owen Rowland (Sept. 2020). „Fatty Acyl Synthetases and Thioesterases in Plant Lipid Metabolism: Diverse Functions and Biotechnological Applications“. In: *Lipids* 55.5, pp. 435–455.

- Kato, Tadahiro, Chizuko Kabuto, Nobuki Sasaki, Mitsuaki Tsunagawa, Hiroyashu Aizawa, Kenichi Fujita, Yoshiaki Kato, Yoshio Kitahara, and Norindo Takahashi (1973). „Momilactones, growth inhibitors from rice, *Oryza sativa* L.“ In: *Tetrahedron Letters* 14.39, pp. 3861–3864.
- Kato-Noguchi, Hisashi (Apr. 2023). *Defensive Molecules Momilactones A and B: Function, Biosynthesis, Induction and Occurrence*.
- Kato-Noguchi, Hisashi, Morifumi Hasegawa, Takeshi Ino, Katsumi Ota, and Hiroya Kujime (July 2010). „Contribution of momilactone A and B to rice allelopathy“. In: *Journal of Plant Physiology* 167.10, pp. 787–791.
- Kato-Noguchi, Hisashi, Takeshi Ino, Noriko Sata, and Shosuke Yamamura (2002). „Isolation and identification of a potent allelopathic substance in rice root exudates“. In: *Physiologia Plantarum* 115.3, pp. 401–405.
- Kato-Noguchi, Hisashi, Seiji Kosemura, and Shosuke Yamamura (1999). „Kato-Noguchi et al. 1999 - A New Inhibitor of Auxin-induced Growth, 5-Chloro-6methoxy-2-benzoxazolinone, from Light-grown Shoots of Maize Seedlings“. In: *Journal of Plant Physiology* 154, pp. 102–105.
- Kato-Noguchi, Hisashi, Katsumi Ota, and Hiroya Kujime (Oct. 2012). „Absorption of momilactone A and B by *Arabidopsis thaliana* L. and the growth inhibitory effects“. In: *Journal of Plant Physiology* 169.15, pp. 1471–1476.
- Kitaoka, Naoki, Juan Zhang, Richard K. Oyagbenro, Benjamin Brown, Yisheng Wu, Bing Yang, Zhaohu Li, and Reuben J. Peters (Feb. 2021). „Interdependent evolution of biosynthetic gene clusters for momilactone production in rice“. In: *Plant Cell* 33.2, pp. 290–305.
- Kumar, Narendra, Hukum Singh, Krishna Giri, et al. (Mar. 2024). „Physiological and molecular insights into the allelopathic effects on agroecosystems under changing environmental conditions“. In: *Physiology and Molecular Biology of Plants* 30.3, pp. 417–433.
- Kumar, Rajesh, Lam Son Phan Tran, Anjanasree K. Neelakandan, and Henry T. Nguyen (Feb. 2012). „Higher plant cytochrome b5 polypeptides modulate fatty acid desaturation“. In: *PLoS ONE* 7.2.
- Liu, Chang Jun (Sept. 2022). „Cytochrome b5: A versatile electron carrier and regulator for plant metabolism“. In: *Frontiers in Plant Science* 13.
- Lu, Yufang, Xiaonan Zhang, Mingkun Ma, Weijun Zu, Herbert J. Kronzucker, and Weiming Shi (Apr. 2022). „Syringic acid from rice as a biological nitrification and urease inhibitor and its synergism with 1,9-decanediol“. In: *Biology and Fertility of Soils* 58.3, pp. 277–289.

- Ma, Xiaoli, Haifeng Xu, Yuru Tong, Yunfeng Luo, Qinghua Dong, and Tao Jiang (Dec. 2023). „Structural and functional investigations of syn-copalyl diphosphate synthase from *Oryza sativa*“. In: *Communications Chemistry* 6.1, pp. 1–14.
- Maharjan, Bal, Stanislav Vitha, and Sakiko Okumoto (Aug. 2023). „Developmental regulation and physical interaction among enzymes involved in sorgoleone biosynthesis“. In: *Plant Journal* 115.3, pp. 820–832.
- Mao, Lingfeng, Hiroshi Kawaide, Toshiya Higuchi, et al. (2020). „Genomic evidence for convergent evolution of gene clusters for momilactone biosynthesis in land plants“. In: *PNAS* 117.22, pp. 12472–12480.
- Moon, Ki Beom, Ji Sun Park, Youn Il Park, In Ja Song, Hyo Jun Lee, Hye Sun Cho, Jae Heung Jeon, and Hyun Soon Kim (Jan. 2020). „Development of systems for the production of plant-derived biopharmaceuticals“. In: *Plants* 9.30, pp. 1–21.
- Mwamahonje, Andekelile, John Saviour Yaw Eleblu, Kwadwo Ofori, Santosh Deshpande, Tileye Feyissa, and Pangirayi Tongoona (Dec. 2021). „Drought tolerance and application of marker-assisted selection in sorghum“. In: *Biology* 10.12, pp. 1249–1267.
- Nelson, David R. (Jan. 2018). „Cytochrome P450 diversity in the tree of life“. In: *Biochimica et Biophysica Acta - Proteins and Proteomics* 1866.1, pp. 141–154.
- Nørholm, Morten H.H. (2010). „A mutant Pfu DNA polymerase designed for advanced uracil-excision DNA engineering“. In: *BMC Biotechnology* 10.21.
- Nour-Eldin, Hussam Hassan, Fernando Geu-Flores, and Barabara Ann Halkier (2010). „USER Cloning and USER Fusion: The Ideal Cloning Techniques for Small and Big Laboratories“. In: *Methods in Molecular Biology* 643, pp. 185–200.
- Okumoto, Sakiko, Bal Maharjan, Nithya Rajan, et al. (May 2025). „Synthesis, function, and genetic variation of sorgoleone, the major biological nitrification inhibitor in sorghum“. In: *Crop Science* 65.3.
- Oliveira, Isabela Figueiredo de, Talita Camargos Gomes, Maria Lucia Ferreira Simeone, Decio Karam, and Sylvia Morais de Sousa Tinoco (Sept. 2024). „Sorgoleone unveiled: exploring its biosynthesis, functional perspectives and applications“. In: *Brazilian Journal of Botany* 47.3, pp. 723–733.
- Ono, Eiichiro and Jun Murata (Dec. 2023). „Exploring the Evolvability of Plant Specialized Metabolism: Uniqueness Out Of Uniformity and Uniqueness Behind Uniformity“. In: *Plant and Cell Physiology* 64.12, pp. 1449–1465.
- Otaka, Junnosuke, Guntur Venkata Subbarao, Hiroshi Ono, and Tadashi Yoshihashi (Apr. 2022). „Biological nitrification inhibition in maize—isolation and identification of hydrophobic inhibitors from root exudates“. In: *Biology and Fertility of Soils* 58.3, pp. 251–264.

- Otomo, Kazuko, Yuri Kanno, Akihiro Motegi, et al. (2004). „Diterpene Cyclases Responsible for the Biosynthesis of Phytoalexins, Momilactones A, B, and Oryzalexins A-F in Rice“. In: *Bioscience, Biotechnology, and Biochemistry* 68.9, pp. 2001–2006.
- Pan, Zhiqiang, Scott R. Baerson, Mei Wang, et al. (Apr. 2018). „A cytochrome P450 CYP71 enzyme expressed in Sorghum bicolor root hair cells participates in the biosynthesis of the benzoquinone allelochemical sorgoleone“. In: *New Phytologist* 218.2, pp. 616–629.
- Pan, Zhiqiang, Joanna Bajsa-Hirschel, Justin N. Vaughn, Agnes M. Rimando, Scott R. Baerson, and Stephen O. Duke (Apr. 2021). „In vivo assembly of the sorgoleone biosynthetic pathway and its impact on agroinfiltrated leaves of Nicotiana benthamiana“. In: *New Phytologist* 230.2, pp. 683–697.
- Pan, Zhiqiang, Agnes M. Rimando, Scott R. Baerson, Mark Fishbein, and Stephen O. Duke (Feb. 2007). „Functional characterization of desaturases involved in the formation of the terminal double bond of an unusual 16:3Δ9,12,15 fatty acid isolated from Sorghum bicolor root hairs“. In: *Journal of Biological Chemistry* 282.7, pp. 4326–4335.
- Peremarti, Ariadna, Richard M. Twyman, Sonia Gómez-Galera, et al. (July 2010). „Promoter diversity in multigene transformation“. In: *Plant Molecular Biology* 73.4, pp. 363–378.
- Peterson, Mark A., Steve A. McMaster, Dean E. Riechers, Josh Skelton, and Phillip W. Stahlman (June 2016). „2,4-D Past, Present, and Future: A Review“. In: *Weed Technology* 30.2, pp. 303–345.
- Phillips, Michael A., Patricia León, Albert Boronat, and Manuel Rodríguez-Concepción (Dec. 2008). „The plastidial MEP pathway: unified nomenclature and resources“. In: *Trends in Plant Science* 13.12, pp. 619–623.
- Pingali, Prabhu L. (July 2012). „Green revolution: Impacts, limits, and the path ahead“. In: *Proceedings of the National Academy of Sciences of the United States of America* 109.31, pp. 12302–12308.
- Priego-Cubero, Santiago, Youming Liu, Tomonobu Toyomasu, Michael Gigl, Yuto Hasegawa, Hideaki Nojiri, Corinna Dawid, Kazunori Okada, and Claude Becker (Mar. 2025). „Evolution and diversification of the momilactone biosynthetic gene cluster in the genus Oryza“. In: *New Phytologist* 245.6, pp. 2681–2697.
- Sáiz-Bonilla, María, Andrea Martín Merchán, Vicente Pallás, and Jose Antonio Navarro (Oct. 2022). „Molecular characterization, targeting and expression analysis of chloroplast and mitochondrion protein import components in Nicotiana benthamiana“. In: *Frontiers in Plant Science* 13.
- Schütz, Vadim, Katharina Frindte, Jiaxin Cui, Pengfan Zhang, Stéphane Hacquard, Paul Schulze-Lefert, Claudia Knief, Margot Schulz, and Peter Dörmann (May 2021).

- „Differential Impact of Plant Secondary Metabolites on the Soil Microbiota“. In: *Frontiers in Microbiology* 12.
- Smil, Vaclav (2001). *Enriching the Earth: Fritz Haber, Carl Bosch, and the Transformation of World Food Production*. 1st. Cambridge, Mass: MIT Press, pp. 61–154.
- Soni, Aditya Prakash, Juhee Lee, Kunyoo Shin, Hisashi Koiwa, and Inhwan Hwang (May 2022). „Production of Recombinant Active Human TGF β 1 in Nicotiana benthamiana“. In: *Frontiers in Plant Science* 13.
- Subbarao, G V, K Nakahara, M P Hurtado, et al. (Oct. 2009). „Evidence for biological nitrification inhibition in Brachiaria pastures“. In: *PNAS* 106.41, pp. 17302–17307.
- Subbarao, G. V., T. Ishikawa, O. Ito, K. Nakahara, H. Y. Wang, and W. L. Berry (Oct. 2006). „A bioluminescence assay to detect nitrification inhibitors released from plant roots: A case study with Brachiaria humidicola“. In: *Plant and Soil* 288.1-2, pp. 101–112.
- Subbarao, G. V., K. Nakahara, T. Ishikawa, et al. (May 2013). „Biological nitrification inhibition (BNI) activity in sorghum and its characterization“. In: *Plant and Soil* 366, pp. 243–259.
- Subbarao, G. V., Ban Tomohiro, Kishii Masahiro, et al. (Oct. 2007). „Can biological nitrification inhibition (BNI) genes from perennial Leymus racemosus (Triticeae) combat nitrification in wheat farming?“ In: *Plant and Soil* 299.1-2, pp. 55–64.
- Tian, Hanqin, Rongting Xu, Josep G. Canadell, et al. (Oct. 2020). „A comprehensive quantification of global nitrous oxide sources and sinks“. In: *Nature* 586.7828, pp. 248–256.
- Trunschke, Judith, Klaus Lunau, Graham H. Pyke, Zong Xin Ren, and Hong Wang (July 2021). „Flower Color Evolution and the Evidence of Pollinator-Mediated Selection“. In: *Frontiers in Plant Science* 12.
- Turusov, Vladimir, Valery Rakitsky, and Lorenzo Tomatis (2002). „Dichlorodiphenyl-trichloroethane (DDT): Ubiquity, Persistence, and Risks“. In: *Environmental Health Perspectives* 110.2, pp. 125–128.
- Ube, Naoki, Yuhka Katsuyama, Keisuke Kariya, Shin ichi Tebayashi, Masayuki Sue, Takuji Tohnooka, Kotomi Ueno, Shin Taketa, and Atsushi Ishihara (Apr. 2021). „Identification of methoxylchalcones produced in response to CuCl₂ treatment and pathogen infection in barley“. In: *Phytochemistry* 184.
- United Nations (Sept. 2025). „Food security and nutrition and sustainable agriculture“. In: <https://sdgs.un.org/topics/food-security-and-nutrition-and-sustainable-agriculture> Accessed: 16/09/2025.
- Vasav, A. P. and V. T. Barvkar (Feb. 2019). „Phylogenomic analysis of cytochrome P450 multigene family and their differential expression analysis in Solanum lycopersicum L. suggested tissue specific promoters“. In: *BMC Genomics* 20.1.

- Voinnet, Olivier, Susana Rivas, Pere Mestre, and David Baulcombe (Mar. 2003). „An enhanced transient expression system in plants based on suppression of gene silencing by the p19 protein of tomato bushy stunt virus“. In: *Plant Journal* 33.5, pp. 949–956.
- Wang, Peng, Yen Ning Chai, Rebecca Roston, Franck E Dayan, Daniel P Schachtman, and Citation P Wang (2021). „The Sorghum bicolor Root Exudate Sorgoleone Shapes Bacterial Communities and Delays Network Formation“. In: *mSystems* 6.2.
- Wei, Kaifa and Huiqin Chen (Jan. 2018). „Global identification, structural analysis and expression characterization of cytochrome P450 monooxygenase superfamily in rice“. In: *BMC Genomics* 19.35.
- Werck-Reichhart, Danièle (Feb. 2023). „Promiscuity, a Driver of Plant Cytochrome P450 Evolution?“ In: *Biomolecules* 13.2.
- Weston, Leslie A., Ibrahim S. Alsaadawi, and Scott R. Baerson (Feb. 2013). „Sorghum Allelopathy-From Ecosystem to Molecule“. In: *Journal of Chemical Ecology* 39.2, pp. 142–153.
- Wu, Dongya, Yiyu Hu, Shota Akashi, Hideaki Nojiri, Longbiao Guo, Chu Yu Ye, Qian Hao Zhu, Kazunori Okada, and Longjiang Fan (Sept. 2022). „Lateral transfers lead to the birth of momilactone biosynthetic gene clusters in grass“. In: *Plant Journal* 111.5, pp. 1354–1367.
- Xu, Meimei, Matthew L. Hillwig, Sladjana Prisic, Robert M. Coates, and Reuben J. Peters (Aug. 2004). „Functional identification of rice syn-copalyl diphosphate synthase and its role in initiating biosynthesis of diterpenoid phytoalexin/allelopathic natural products“. In: *The Plant Journal* 39.3, pp. 309–318.
- Xu, You, Xin Chen, Le Ding, and Chui Hua Kong (Mar. 2023). „Allelopathy and Allelochemicals in Grasslands and Forests“. In: *Forests* 14.3, pp. 562–584.
- Zhao, Huayan, Dylan K. Kosma, and Shiyou Lü (Mar. 2021). „Functional Role of Long-Chain Acyl-CoA Synthetases in Plant Development and Stress Responses“. In: *Frontiers in Plant Science* 12.
- Zhao, Xianhai, Yunjun Zhao, Mingyue Gou, and Chang-Jun Liu (2023). „Tissue-preferential recruitment of electron transfer chains for cytochrome P450-catalyzed phenolic biosynthesis“. In: *Science Advances* 9.

Appendix

Momilactone primers	
Name	5'-3' sequence
OsCYP76M8_USER_Fw	GGCTTAAU ATGGAGAACTCACAAATGTGGC
OsCYP76M8_USER_Rv	GGTTTAAUTTA CTTGATCAATACTGGAACAGC
cytOsKSL4_USER_Fw	GGCTTAAUATG AGTGCTGAGCTGGACACTG
cytOsKSL4_USER_Rv	GGTTTAAUTTA GTTACCTCTGGTCTTGAGAGGC
cytOsCPS4_USER_Fw	GGCTTAAUATG TTGATCAGTAAATCACCACCATACC
cytOsCPS4_USER_Rv	GGTTTAAUTTA AATTACATCCTGGAAAATGACCTTATC
OsMAS_USER_Fw	GGCTTAAU ATGGCCGCTGGTCTTCAC
OsMAS_USER_Rv	GGTTTAAUTTA GTCTCTGAAGAACCGAAGC
OsCYP76M14_USER_Fw	GGCTTAAU ATGGAGAAATCATCAGAACTGTGGC
OsCYP76M14_USER_Rv	GGTTTAAUTTA GTTGATCACCTTAACTGGAACAGC
OsCYP99A3_USER_Fw	GGCTTAAU ATGATGGAGATCAACTCTGAGGC
OsCYP99A3_USER_Rv	GGTTTAAUTTA AGATTGCATGGAGATCGGTTG
OsCYP701A8_USER_Fw	GGCTTAAU ATGGAATCCATGCTTGT CGC
OsCYP701A8_USER_Rv	GGTTTAAUTTA CATCCTCCTCTAGGCTTCAAG
SbCYP76M8_USER_Fw	GGCTTAAU ATGGGAGCTTGTCCCTTG
SbCYP76M8_USER_Rv	GGTTTAAUTTA AATTGCAGTAGCAATAGCACAG
cytSbKSL4_USER_Fw	GGCTTAAUATG GAGTTGAAACAAGAATTAGAAATCAAC
cytSbKSL4_USER_Rv	GGTTTAAUTTA CTTACCGGGATGATGAGGACAAG
SbMAS_USER_Fw	GGCTTAAU ATGGCTGCTGCCGGCAGTT
SbMAS_USER_Rv	GGTTTAAUTTA GTCATCAAATGGACGCAAGTTATGGTTAAC
SbCYP76M14_USER_Fw	GGCTTAAU ATGGGTGCTCTTTCCCATG
SbCYP76M14_USER_Rv	GGTTTAAUTTA ATGGCTGTAGCAATAGCACAG
SbCYP99A3_USER_Fw	GGCTTAAU ATGGAGTTGATCTACTACCACAG
SbCYP99A3_USER_Rv	GGTTTAAUTTA CATTGAACTTGGTATGGAGAAG
SbCYP701A8_USER_Fw	GGCTTAAU ATGGAAAGTTGGTGTGCTGC
SbCYP701A8_USER_Rv	GGTTTAAUTTA CTTCTACCTCTGGAGTCAAGTAG
cPCR_pLIFE33_Fw	TTCATTGGAGAGGAGCACCTG
cPCR_pLIFE33_Rv	CCTTATCTGGGAACTACTCACAC

Table Appendix 1: Momilactone pathway rice gene and sorghum ortholog primers used for cloning of the pLIFE33 tobacco expression vectors used. USER overhang is marked in red, start codons are introduced for truncation of plastid signal peptides denoted in green, and stop codons are denoted in blue. The last two are for running colony PCR using primers in the pLIFE33 vector backbone.

Table Appendix 2: DNA sequences of codon optimized genes used in this study. All genes are codon optimized for *S. cerevisiae* and *N. benthamiana* except the sorgoleone biosynthetic genes that are optimized for *S. cerevisiae* and *Y. lipolytica*.

Continued on next page

Continued on next page

Continued on next page

Continued on next page

Name	5'-3' sequence
SbLACS4.1	<pre> ATGAAAGCATTTAGTCGAAGTTGAAACCGCTACCGCCACCAGTGGCCAGGTACAGAAATGCTAGAGCTAAGGATGCTATTGCAAGCTCCACCGAG TTTGCACTCTGGGGACATCTCAGAACCTCCGTCGAAAAGTACCCAGATAACCCAATGTTGGTAGAAGAAGACTCCTGACGGTAAGGGTTC TGACTACACCTGGGTTACCTACAAGAGGTTATGACGCCATTAGAAGTTACTGCTCTATTGACAAAAGCGTATAAACGAAAGCTGAAGGTGT GGTATCTACGGTGTAACTGTCAGAATGGATTATCTCATGGAAAGCTGTAAAGCTTGGGTGTCGTTGTCATTTACGACTCTTAAAGTGT CGGGTGTGTTGAATTATCATCTCACCGCTGAATTCAGCTTGCAGGAAATCCTGTTGAGAAAGTACTGCTATGCAAGCTTGTGATGCTAC CTCTAAGTACTTGAAGACTGTTATTCTTCGGGTGTCACCAACGATCACAGAGACGAAAGCCAGAAACCATGTTGCTATTTCCTTGGGAA GAATTCTGGTTATCGGGTGTCTCACCACTTCGACTTGCCAGAAAAGAACGACATGCCACATCTGACTGTGACTGTGACTGTGTTACCCGGTG ATGATGCTACTTATCTTACCTGGCTCACGTTGCACTGGCAGAATGTTGCAAGAAAGCTTATTCGCTGTTCCAGGTCTAGACAGAAATTACTCTGTTGA GGTAGTGTAAAGTTGTTGGTGAGGATTTGAAGCTTGAAGCAACCTTATCTGCTGTTCCAGGTCTAGACAGAAATTACTCTGTTGA CTACAGAACTTGTCAACATTTGCTTCAAGGAAACTCTGTCACATGGTAAAGGATGACAAACATGAGAAAGGGTATCAAGCAGA AACTGCTGCTCATCTCGAACAAATGGTCTTCAGAACGTTGGGTGAGAATGTTGATATCTCGGTTGTCACCGTTA GCCGTCCTGTTGAGAATCTCAGTGGTCACTGGTCACTGGTCAAGTGGTCAAGTGGTCAAGTGGTCAAGTGGTCAAGTGGTCAAGTGGT TTCCTAAAGTGAATACTCATGTTGCTTCAGTCCACACATGACTGATAGTGTCAAGTGGTCAAGTGGTCAAGTGGTCAAGTGGTCAAGTGGT GTTGGTCTTCAACTGGTGAATGGGAAACTGGTCAAGGAACTGGTCAAGTGGTCAAGTGGTCAAGTGGTCAAGTGGTCAAGTGGTCAAGTGGT AAATAGCTGCTTCAAGGAACTGGTCAAGGAAACTGGTCAAGTGGTCAAGTGGTCAAGTGGTCAAGTGGTCAAGTGGTCAAGTGGTCAAGTGGT TGCGTTGTTAACCAAACCAAAGGTTAAAGATGGGTGAAATACACATCGTGTCTTGTGAATGTCATGGTCAAGTGGTCAAGTGGTCAAGTGGT AAGGAACACATTATGCGCAATGCGAAATGGCAAGGAAAGTGGTCAAGTGGTCAAGTGGTCAAGTGGTCAAGTGGTCAAGTGGTCAAGTGGT TCGACATTGATCATCTCAACTTAAAGAAGACACAAATGTTAAAGTACTACAGGTTACGATGCTCTATTAAGGTTACGATGCTCTATTAAGAG TATGAAA </pre>
SbMSBP1	<pre> ATGGCTTGTGAAATTGGGAAACTTGAACAAACGATATCGTTGCTTACACTGGTTGCTCCAGGTGTTTAACTGGTGTGCAAGTGTG CTGCATTATACCATGTTGTTCTGTTGTCACCAACCCCTCCACAAAGACCAAGAGAAAGAACGCTGAACCATGGCACCACCC AGTTCAAAAGGGTGTAAAGCTTGAAGGAAATTGAGACAATATGATGGTCCATTACCCAAAAGCCTTGGTGTGATGGCTTAAATGGGTCAAACTCAC GATGTCACCCAACTTGAAGTGTGTTATGGTCAAGGTGTCATATGCTTATTTGCTGTTAAAGATGCTTGTGCTAAAGTGTCTTTG AAACCAAGATTGACTGGTGCACATTCAAGGTTGGTCATTGAAATTGGGACTACAGTCTAGTCTAAAGTGTCTAGTCTAAAGTGTAA GTTGGCACCGTIAAGAAAAGTTCGACTGTTGAAGATGCTTCTACTGCTTCAAGGCTTCAAGGCTAACACTGAAGCTAAAGCTGAAAAGCT CAAACACTGAAGAAAAGCCAAGAGGTTCTGCTGAAGCTCAAGAAAAAGACACAAATGTTAAAGTACTACAGGTTACGATGCTCTATTAAGAG TGGCTGTTGCTGTTGAATGATCAAAGTCTGAGCTGAGCTGTTGCTAAAGAAAAAGCTCATCTGACGAGGTGCCAAGAAAAGCTAA </pre>
SbCytb5.6	<pre> ATGGAACAAAAACTCATCTCAGAACAGGATCTGCTAAAGGTTTACTTGGAAAGATGTTGCTAACGATAACACAAAGGAGATTGGTGGTGTGATTA TTGGTGGAAAGGTTAACGATGTTACTAAGCTCTGAAACATCAGCTAGACCTATGATGATGAAACATCCCTGGAGATGATGTTGCTTGTCTCAACTGGTAAAGATGCTAACAGATGA TTTGAGGATGTTGGACATTCAAAATACAGCTAGACCTATGATGATGATGAAACATCCCTGGAGATGATGTTGCTTGTCTCAACTGGTAAAGATGCTAACAGATGA TATGTCCTCCAAAACACCTATTACAATCAGGATAAGACTCCAGAATTCGTTGAGGATGCTTGTCTCAACTGGTAAAGATGCTAACAGATGA TGACATTGATCATCTCAACTTAAAGAAGACACAAATGTTAAAGTACTACAGGTTACGATGCTCTATTAAGGTTACGATGCTCTATTAAGAG TGGCTGTTGCTGTTGAATGATCAAAGTCTGAGCTGAGCTGTTGCTAAAGAAAAAGCTCATCTGACGAGGTGCCAAGAAAAGCTAA </pre>

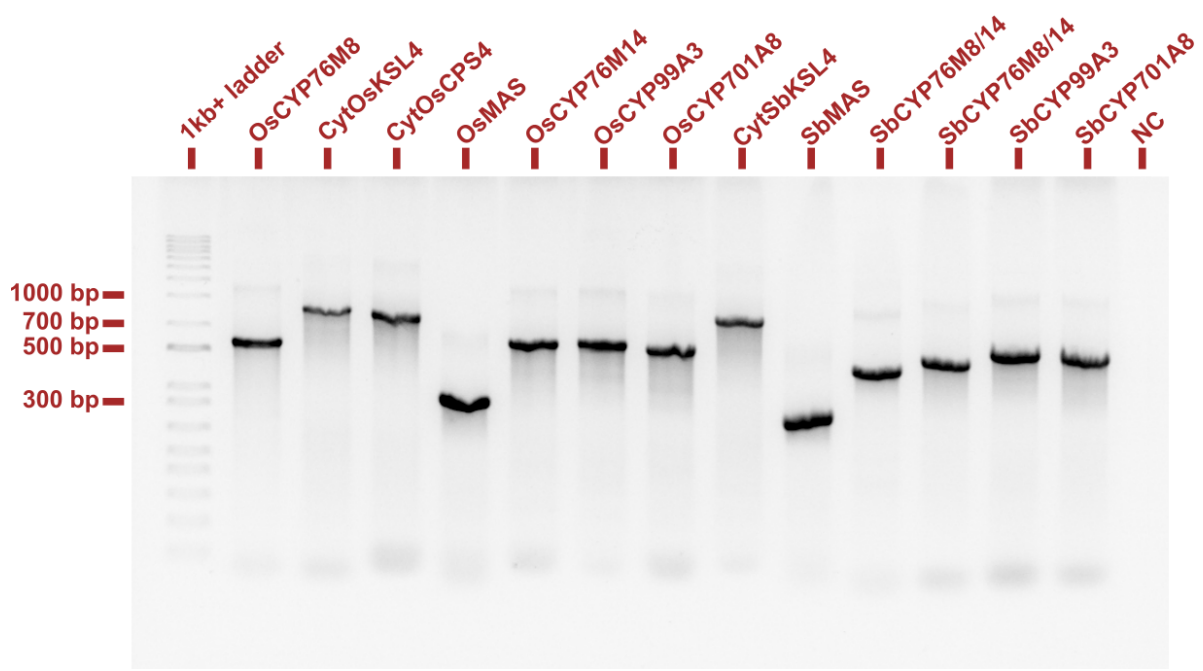


Figure Appendix 1: Gel-electrophoresis visualization of PCR amplicons from the USER cloning preparation of momilactone B biosynthesis genes from rice and sorghum. All amplicons are of the assumed sizes denoted in Tables 1 & 2.

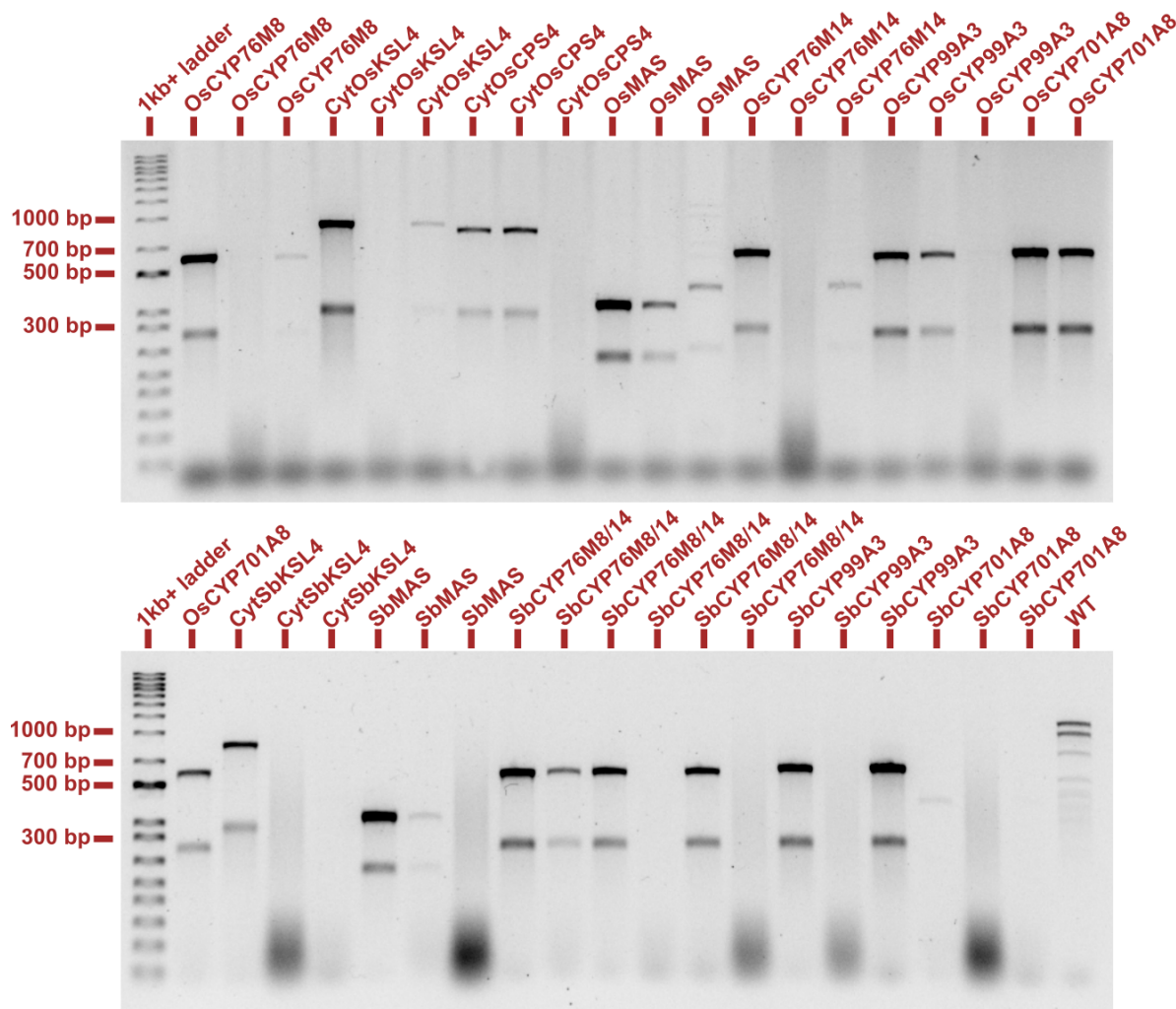


Figure Appendix 2: Gel-electrophoresis visualization of colony PCR amplicons testing for insertion of respective gene fragments in transformation of momilactone B biosynthetic gene plasmids into *E. coli*.

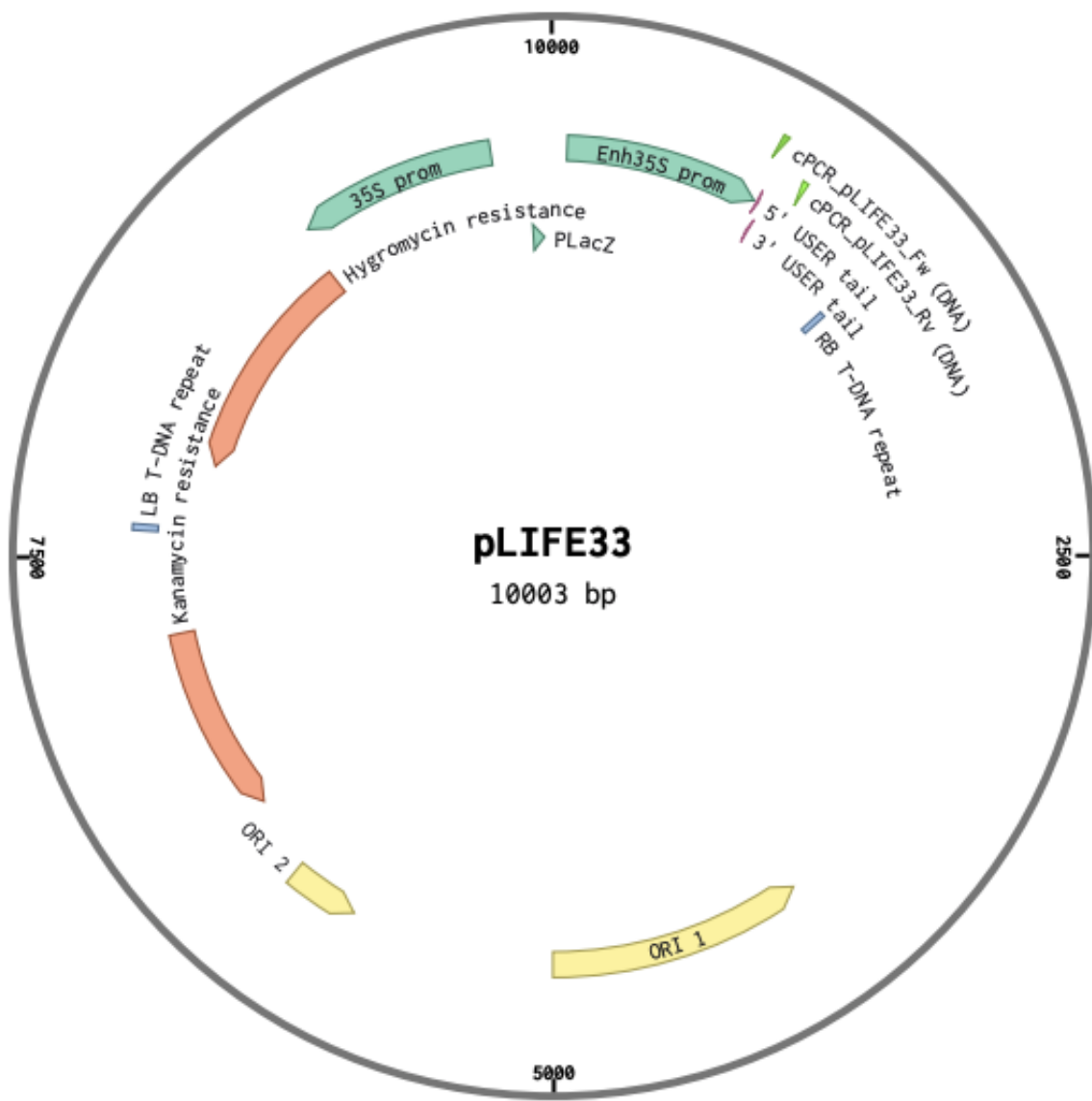


Figure Appendix 3: Plasmid map of pLIFE33 shuttle vector backbone. Gene insertions are made between the 5' and 3' USER tails.

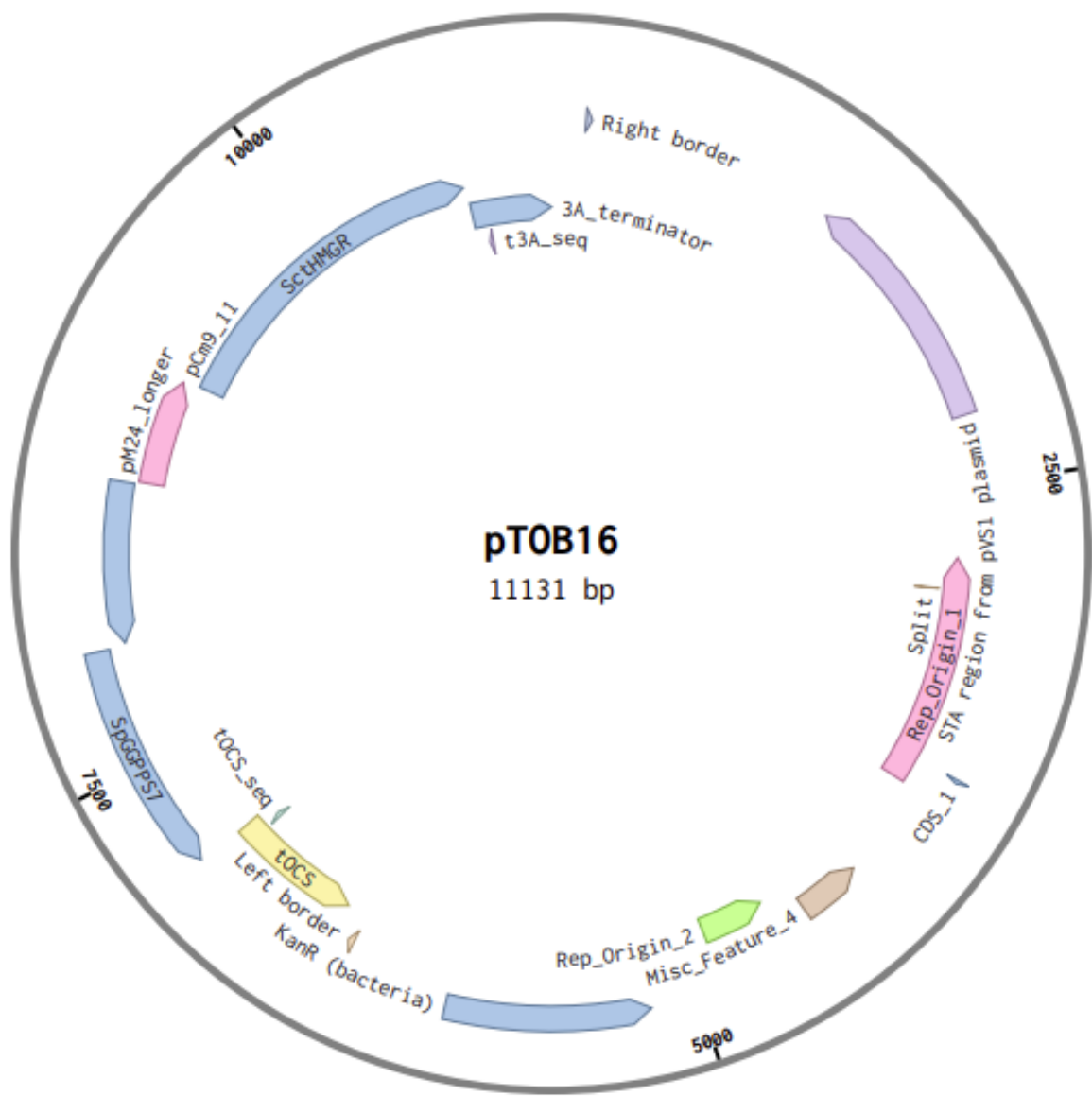


Figure Appendix 4: Plasmid map of pTOB16 harboring SpGGPPS and SctHMGR. Kindly provided by Feiyan Liang.

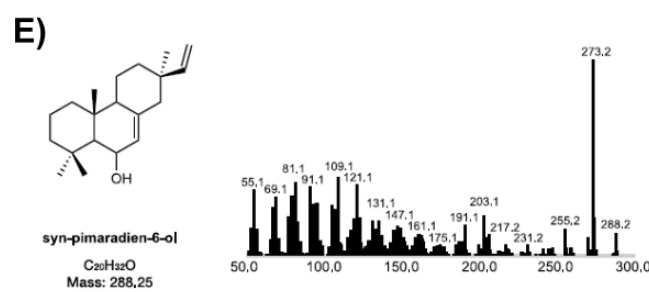
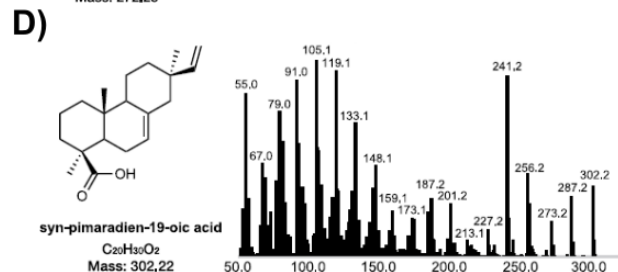
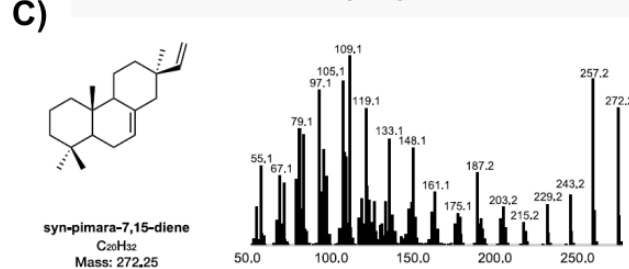
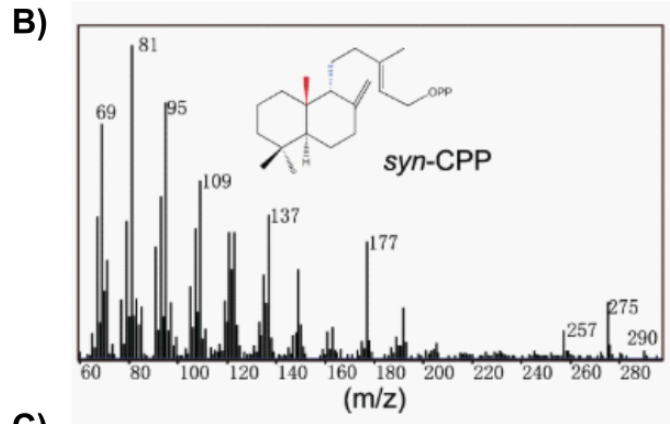
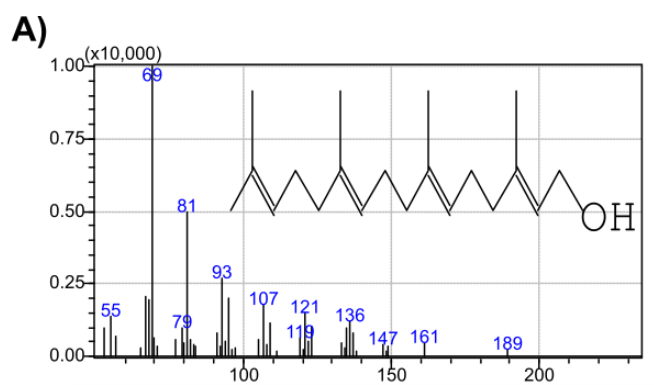


Figure Appendix 5: Reference spectra for A) geranylgeraniol (NIST08 library), B) syn-copalyl hydroxide (Ma *et al.*, 2023), C) syn-pimaradiene (De La Peña and Sattely, 2021), D) syn-pimaradien-19-oic acid (De La Peña and Sattely, 2021), and E) syn-pimaradien-6-ol (De La Peña and Sattely, 2021)

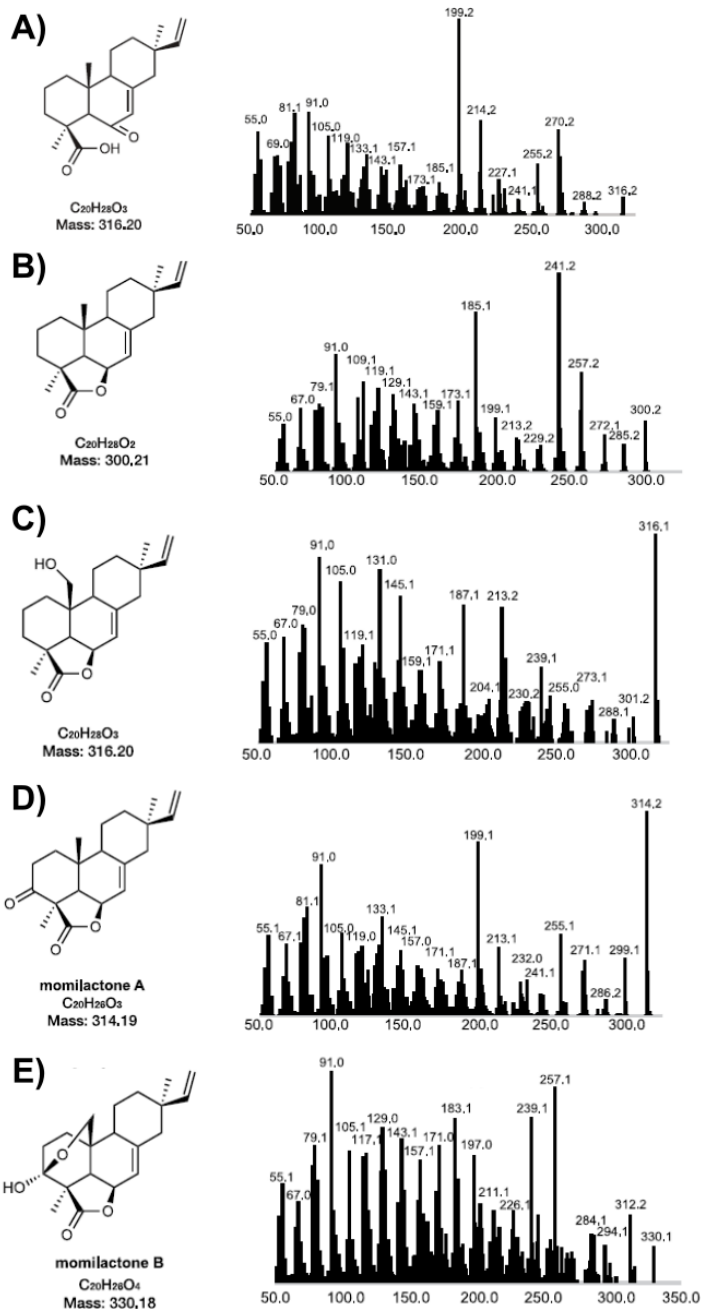


Figure Appendix 6: Reference spectra for A) 6 β -carboxy-synpimaradienon-19-oic acid, B) syn-pimaradienon-19,6 β -olide, C) 20-hydroxy-synpimaradienon-19,6 β -olide, D) momilactone A, and E) momilactone B. All are modified from De La Peña and Sattely (2021).

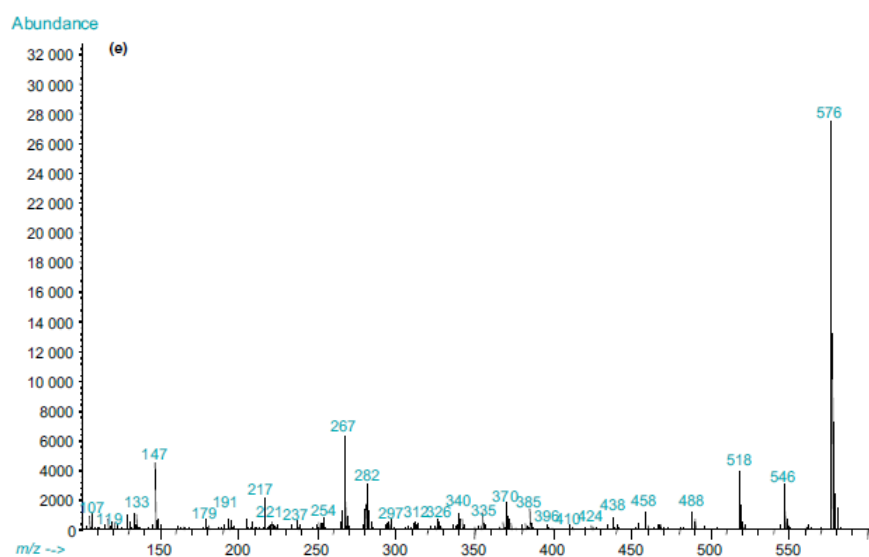


Figure Appendix 7: Reference spectrum for BSTFA derivatized dihydrosorgoleone. Figure is from (Pan *et al.*, 2018).

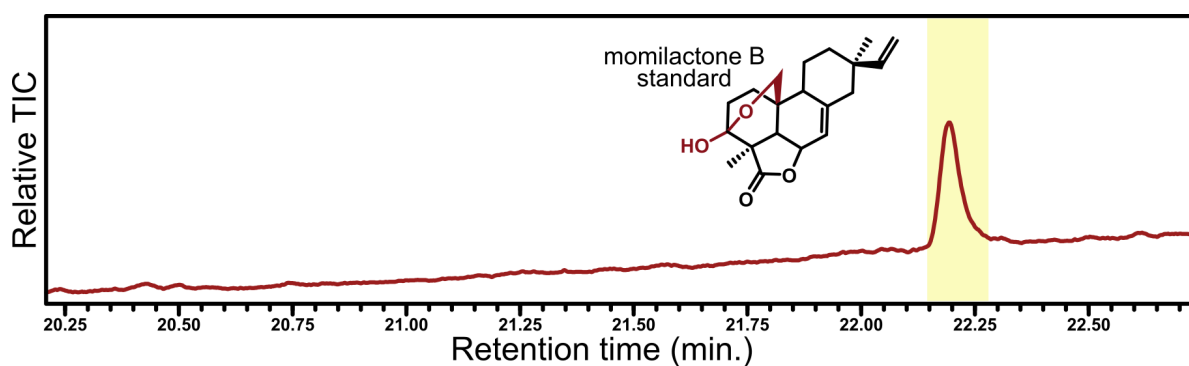


Figure Appendix 8: Total ion chromatogram (TIC) peak of 1mM momilactone B standard.



UCPH's AI declaration

Declaration of using generative AI tools

- I/we have used generative AI as an aid/tool (please tick)
- I/we have NOT used generative AI as an aid/tool (please tick)

If generative AI is permitted in the exam, but you haven't used it in your exam paper, you just need to tick the box stating that you have not used GAI. You don't have to fill in the rest.

List which GAI tools you have used and include the link to the platform (if possible):

Perplexity - <https://www.perplexity.ai/>

ChatGPT5 - <https://chatgpt.com/>

Describe how generative AI has been used in the exam paper:

Used LLMs as a sparring partner to acquire knowledge for the generation and understanding of protocols for laboratory experiments. They were also used in the ideation phase of setting up the overall structure of the thesis with regards to maintaining the red thread throughout. They were also used in literature search, to quickly find review papers and relevant research on different topics of interest.

Please note: Content generated by GAI that is used as a source in the paper requires correct use of quotation marks and source referencing. Read the guidelines from Copenhagen University Library at KUnet [here](#).